nature microbiology

SUPPLEMENTARY INFORMATION

https://doi.org/10.1038/s41564-019-0406-9

In the format provided by the authors and unedited.

Proposal of the reverse flow model for the origin of the eukaryotic cell based on comparative analyses of Asgard archaeal metabolism

Anja Spang[1,2]*, Courtney W. Stairs[1], Nina Dombrowski[2,3], Laura Eme[1], Jonathan Lombard[1], Eva F. Caceres[1], Chris Greening[4], Brett J. Baker[3] and Thijs J. G. Ettema[1,5]*

[1]Department of Cell and Molecular Biology, Science for Life Laboratory, Uppsala University, Uppsala, Sweden. [2]NIOZ, Royal Netherlands Institute for Sea Research, Department of Marine Microbiology and Biogeochemistry, and Utrecht University, AB Den Burg, The Netherlands. [3]Department of Marine Science, University of Texas at Austin, Marine Science Institute, Port Aransas, TX, USA. [4]School of Biological Sciences, Monash University, Clayton, Victoria, Australia. [5]Laboratory of Microbiology, Department of Agrotechnology and Food Sciences, Wageningen University, Wageningen, The Netherlands. *e-mail: anja.spang@nioz.nl; thijs.ettema@wur.nl

Supplementary Information for

Proposal of the reverse flow model for the origin of the eukaryotic cell based on comparative analysis of Asgard archaeal metabolism

Anja Spang[1,2], Courtney Stairs[1], Nina Dombrowski[3], Laura Eme[1], Jonathan Lombard[1], Eva Fernández Cáceres[1], Chris Greening, Brett J. Baker[3] and Thijs J. G. Ettema[1]

Table of contents

A. Supplementary text

1. Carbon metabolism and the potential for autotrophic carbon fixation

Central Carbon metabolism. All members of the Asgard archaea contain candidate genes encoding enzymes for most steps of glycolysis via the Embden-Meyerhof-Parnas (EMP) pathway as well as gluconeogenesis and the tricarboxylic acid cycle (TCA; Suppl. Tables 1 and 2, Suppl. Figure 2). However, the specific enzymes catalyzing these steps differ among the various lineages (Suppl. Tables 1 and 2). For example, our analysis of enzymes potentially involved in glycolysis revealed that only three members of the Asgard archaea appear to encode enzymes belonging to described hexo- or glucokinase families: the archaeal ADP-dependent phosphofructokinase/glucokinase in the two Heimdallarchaeota LC3 and AB125 (PF04587) and a ROK (repressor, open reading frame, kinase) family enzyme in *Lokiarchaeum* GC14-75 (PF00480) (Suppl. Table 2), which could potentially phosphorylate glucose and thus perform the first step of the EMP pathway. While all genomes encode various proteins with phosphofructokinase (Pfk) B family carbohydrate kinase (PF00294) or FGGY family of carbohydrate kinase domains (PF02782)[1], it is currently unclear whether some of those proteins could represent new kinase families acting on glucose as substrate. Additionally, *Odinarchaeum* lacks candidate genes for a phosphoglucose isomerase (EC 5.3.1.8/9) and phosphofructokinase (EC 2.7.1.11/ 2.7.1.146). It is also interesting to note that genes for the bifunctional archaeal fructose-1,6-bisphosphate aldolase/phosphatase (FBPA/FBPase), which has been suggested to represent an ancient carbon fixation enzyme in archaea[2], could not be identified in the genomes of Lokiarchaeota and two Heimdallarchaeota (while present in the other Asgard genomes). However, these organisms (except *Lokiarchaeum* CR4) could perhaps catalyze this reaction in two steps using a fructose-bisphosphate aldolase and an archaeal fructose-1,6-bisphosphatase (Suppl. Tables 1 and 2, Suppl. Figure 2).

The TCA is nearly complete in most Asgard genomes (Suppl. Figure 2, Suppl. Tables 1 and 2) except *Odinarchaeum* and perhaps *Lokiarchaeum* CR_4, which lack genes for all subunits of a succinyl-CoA synthetase (EC 6.2.1.5) and for a succinate dehydrogenase/fumarate reductase (EC 1.3.5.1/4). Several genomes lack genes for canonical malate dehydrogenases as well as a membrane-bound malate:quinone-oxidoreductase (IPR006231), which catalyze the oxidation of malate to oxaloacetate (Suppl. Figure 2). However, in those organisms, malate could be converted to pyruvate using malic enzyme (EC 1.1.1.38/40).

Interestingly, the gene repertoire coding for proteins involved in ribose sugar metabolism and the corresponding pathways vary substantially across Asgard lineages (Fig. 1, Suppl. Tables 1 and 2). While Lokiarchaeota (both lineages), *Heimdallarchaeum* AB125 and *Odinarchaeum* seem to use the ribulose-5-phosphate pathway, genomes of Thorarchaeota appear to encode genes for enzymes of the non-oxidative pentose phosphate (PP) pathway and *Heimdallarchaeum* LC2 and LC3 might employ the oxidative PP pathway (Fig. 1, Suppl. Tables 1 and 2). Notably, the *Odinarchaeaum* genome lacks genes for ribose 5-phosphate isomerase (both Type A (IPR004788) and B (IPR003500, IPR004785) enzymes), which reversibly converts D-ribulose 5-phosphate to D-ribose 5-phosphate. Since D-ribose 5-phosphate represents a precursor for nucleotide biosynthesis[3], a homologue of this enzyme, i.e. of

Type A, is encoded by most archaeal genomes independent of whether the respective organisms employ the PP- or ribulose monophosphate (RuMP)-pathway. Prospective genomic analyses of additional members of these archaea is needed to determine whether these patterns reflect different catabolic and anabolic abilities or are a result of genome bin incompleteness.

Wood-Ljungdahl pathway. In accordance with previous analyses[4-6], we could identify genes for all enzymes of the Wood-Ljungdahl pathway (WLP)[7,8] in Loki- and Thorarchaeota (Suppl. Figure 2). In particular, these genomes encode the archaeal methyl-branch and carbamoyl-branch as well as the key enzyme CO dehydrogenase/acetyl-CoA synthase (ACS/CODH), which is comprised of five subunits (CdhA-E) and links the two branches by synthesizing acetyl-CoA from carbon monoxide and methyl-H_4MPT via the methylated corrinoid Fe-S protein CH_3-Co(III)FeSP (Suppl. Figure 2, Suppl. Tables 1 and 2)[8]. In contrast, genomes of Heimdallarchaeota do not seem to encode any of the enzymes involved in this pathway. While the genome of the sole representative of the Odinarchaeota encodes genes for the five steps of the methyl-branch leading to the generation of methyl-H_4MPT, it appears to lack genes for all subunits of ACS/CODH (CdhABCDE). In methanogenic archaea, methyl-H_4MPT not only plays a role in carbon fixation but is also the key intermediate in methanogenesis[9]. As such, methyl-H_4MPT is converted to methyl-CoM and subsequently disproportionated to methane and CO_2 by the tetrahydromethanopterin S-methyltransferase complex (Mtr) and methyl-CoM reductase (Mcr), respectively. However, we could not detect genes coding for the eight subunits of the Mtr complex or the five subunits of Mcr in any of the investigated Asgard archaea (see below). This suggests that Loki- and Thorarchaeota are not able to perform methanogenesis, although the use of methylated substrates cannot be excluded (see below). Instead they may use the WLP for autotrophic carbon fixation and perhaps for energy conservation using inorganic (at least Thorarchaeota) and/or organic substrates (Fig. 1). In addition, the WLP could serve as electron sink and thereby allow energetically efficient fermentative growth on various organic substrates (see below) or function in reverse for the complete oxidation of organic substrates[7,10]. Given the lack of ACS/CODH as well as key enzymes of methanogenesis in Odinarchaeota, the functional role of the enzymes of the methyl-branch in this organism remain unknown. However, it should be noted that we can currently not exclude the possibility that the absence of the respective genes is due to genome incompleteness.

Genes encoding for proteins related to methanogenesis. Surprisingly, genomes of Loki-, Thor- and even Heimdallarchaeota encode various proteins assigned to the uroporphyrinogen decarboxylase (URO-D) protein family (IPR000257) (Suppl. Figure 2, Suppl. Tables 1 and 2), which includes candidate proteins for methylcobalamin:coM methyltransferases. Furthermore, each of these genomes encodes at least one protein assigned to the trimethylamine:corrinoid methyltransferase family and *Thorarchaeum* SMTZ1-45 in addition contains a gene coding for a putative monomethylamine methyltransferase. Methyltransferases belonging to these protein families allow several methanogenic archaea to grow on methylated compounds such as methyl sulfides, methylamines and methanol[11]. Notably, homologues of these enzymes encoded by genomes of methanogenic archaea generally

contain the amino acid pyrrolysine, which is thought to be essential for catalysis[12]. However, these methyltransferase families are extremely diverse and not restricted to organisms that encode pyrrolysine. For instance, a trimethylamine:corrinoid methyltransferase that does not contain pyrrolysine has been shown to function as glycine betaine methyltransferase in the gram-positive *Desulfitobacterium hafniense*[13]. Since Asgard archaea seem to lack genes coding for pyrrolysine, their putative trimethylamine:corrinoid methyltransferase may demethylate substrates other than trimethylamine. Methyl-groups could be transferred to corrinoid proteins, candidates for which (COG05012) are encoded by genomes several Asgard genomes (Suppl. Table 2). Corrinoid proteins are involved in methyl-transfer and act as substrate for the methylcobalamin:coenzyme M methyltransferase (IPR000257) leading to the formation of methyl-CoM in methanogens[11]. Lokiarchaeota and Thorarchaeota not only contain genes coding for various proteins assigned to IPR000257 (corrinoid proteins and methyltransferases), but their genomes also reveal the organization of these genes in gene clusters. This suggests that at least Loki- and Thorarchaeota have the ability to convert specific methylated compounds to methyl-CoM. In methanogenic archaea, methyl-CoM is further converted to methane by the key enzyme of methanogenesis: methyl-CoM reductase (Mcr)[11]. However, in contrast to archaea known to be able to use methylated compounds, all herein studied members of the Asgard archaea lack gene homologues coding for the five subunits of Mcr. Furthermore, their genomes do not encode all eight subunits of the membrane-bound tetrahydromethanopterin S-methyltransferase (MtrA-H), which performs a central energy-conserving and sodium-ion-translocating step during methanogenesis and links the methyl-branch of the WLP to methane generation from methyl-CoM. Yet, genomes of Loki-, Odin- and Thorarchaeota encode the methyltransferase subunit MtrH (Suppl. Table 2), which also occurs in various non-methanogenic archaeal and bacterial lineages[14] and has been suggested to also mediate the transfer of a methyl-group between methylcobalamin and tetrahydrofolate[13]. In contrast, in methanogens the methyl-group is transferred to tetrahydromethanopterin via the corrinoid prosthetic group of MtrA[15]. Interestingly, in the different Thorarchaeota, one to two genes coding for MtrH are located in gene clusters with genes encoding MtrA homologues as well as a protein of unknown function related to methanogenesis marker protein 14 (IPR008303). This gene cluster is reminiscent of the *mtr*XAH operon of *Methanosarcina barkeri*, which was suggested to play a role in the methyl-transfer from methylated substrates to tetrahydromethanopterin[16]. It therefore seems possible that at least in Thorarchaeota, MtrH and MtrA homologues may provide a link between Methyl-CoM and Methyl-H_4MPT and/or Methyl-H4F[a] and allow the use of methylated compounds by these archaea.

3-hydroxypropionate/4-hydroxybutyrate cycle. In addition to genes for the WLP, genomes of Loki- and Thorarchaeota but also Heimdallarchaeota encode several enzymes characteristic of the 3-hydroxypropionate/4-hydroxybutyrate (3H4H) carbon fixation pathway (Suppl. Table 1). However, in *Archaeoglobus lithotrophicus,* whose genome also encodes multiple carbon fixation pathways[17], these proteins are involved in the degradation of fatty

[a] Methyl-H4F represents a key intermediate of the methyl-branch in the bacterial-type WLP, genes of which were also identified in Asgard genomes and may encode enzymes functioning in folate biosynthesis (Suppl. Figure 2).

acids and hydrocarbons. It is likely that these enzymes perform similar functions in the Loki-, Thor- and Heimdallarchaeota. For instance, some of the genes encoding these enzymes co-occur with genes for β-oxidation related proteins and are absent in the genome of *Odinarchaeum*, which also lacks genes coding for β-oxidation-related proteins. Furthermore, in *Lokiarchaeum* GC14_75 and *Heimdallarchaeota* LC2 and LC3, some of these genes are encoded in the same region of the chromosome (Suppl. Table 3). For example, in *Lokiarchaeum* GC14_75, methylmalonyl-CoA mutase (COG2185 and COG1884) can be found within two genes of the short chain dehydrogenase gene (ACAD, COG1960, discussed below). Altogether, this supports the idea that these proteins could be involved in the degradation of fatty acids and hydrocarbons in several Asgard archaea.

Calvin-Benson-Bassham Cycle. Furthermore, genomes of all members of the Asgard archaea encode a protein belonging to the ribulose 1,5-bisphosphate carboxylase family (RuBisCO), the key carbon fixation enzyme of the Calvin-Benson-Bassham (CBB) cycle (Suppl. Figure 18a), which adds CO_2 to ribulose 1,5-bisphosphate (RuBP). Our phylogenetic analyses classify a homologue of each of the analysed Thorarchaeota and Lokiarchaeota as Type-IV Rubisco, which is not known to have canonical RuBisCO activity and may instead act on analogous compounds (Suppl. Figure 18a)[18]. In agreement with this, key residues of the active site[19] are not conserved (Suppl. Figure 18b) in most of these Type-IV sequences. However, genomes of *Heimdallarchaeum* AB125, *Lokiarchaeum* CR4, *Lokiarchaeum* GC14_75 and *Heimdallarchaeum* LC3 encode homologues that affiliate either with Type-III RuBisCO or lack clear affiliation, and retain all essential active site residues (Suppl. Figure 18b, except for some with one mutation that maintains the hydrophobicity of the respective amino acid side chain). Thus, those sequences may act as *bona fide* RuBisCO enzymes. However, further research is needed to elucidate the functional context in which these proteins operate. For example, it is possible that they are involved in an AMP salvage pathway[20] (Suppl. Tables 1 and 2), like in *Thermococcus kodakarensis*, rather than in carbon fixation. This is supported by the presence of candidate genes of the AMP salvage pathway in these genomes, i.e. genes coding for a putative AMP phosphorylase as well as a ribose-1,5-bisphosphate isomerase (Suppl. Tables 1 and 2) as well as by the lack of genes encoding additional key enzymes of the CBB and the related carbon fixation pathway referred to as the reductive hexulose-phosphate (RHP) pathway[21]. For example, proteins with the signature domain for phosphoribulokinase (IPR006082), another key enzyme of RuBisCO-based carbon fixation pathways, are not encoded by Asgard genomes. While, *Heimdallarchaeota* LC2 and LC3 do encode enzymes belonging the broader phosphoribulokinase/uridine kinase family (IPR006083; Suppl. Table 2), these seem to represent uridine kinases rather than phosphoribulokinases as they lack the signal domain of and are only distantly related to known phosphoribulokinases (e.g. the use of known phophoribulokinases of *Synechococcus elongatus* (Q31PL2) and *Methanospirillum hungatei* (Q2FUB5) as query against the heimdallarchaeal genomes did not recover a significant hit). Finally, the RuBisCO homologues of *Odinarchaeum* LCB_4 and *Heimdallarchaeum* LC2 have two mutations within the active site residues (Suppl. Figure 18b) and it is therefore unlikely that the corresponding enzymes have retained the canonical carboxylase activity.

2. Asgard archaea have the potential to use various substrates as carbon source including hydrocarbons

The genomes of all Asgard archaea reveal the potential for the degradation of various substrates including complex carbohydrates as evidenced by various carbon active enzymes, peptidases and esterases as well as amino acids (Suppl. Table 4). Also notable is the large variety of paralogues encoding key enzymes of the β-oxidation pathway in all Asgard archaea except for *Odinarchaeum*, which may enable these organisms to use fatty acids of varying chain lengths as carbon source. In addition, Loki- and Thorarchaeota genomes encode putative archaeal formate dehydrogenases (Suppl. Tables 1 and 2), suggesting that these organisms are able to also use formate as a carbon and electron source, enabling the reduction of cofactor F420. Reduced F420 could subsequently allow carbon fixation via the WLP (Fig. 1). Alternatively, the formate dehydrogenase could be used for the generation of formate from CO_2 during the complete oxidation of organic substrates such as fatty acids via the WLP. This may require growth with syntrophic formate-utilizing partner organisms, that would lower the concentration of formate[22]. Altogether, the potential of using organic substrates for growth is in agreement with a higher relative abundance of Lokiarchaeota (DSAG) in organic-rich sediment layers[23,24].

Carbohydrate active enzymes and peptidases. Each Asgard archaea genome has the genetic potential to degrade complex substrates and together they encode 532 carbohydrate-active enzymes (CAZYmes), 338 peptidases and 128 ESTHERs (ESTerases and alpha/beta-Hydrolase Enzymes and Relatives; Suppl. Table 4). Overall, the genome of *Odinarchaeum* LCB_4 encodes for the fewest CAZYmes (24), peptidases (14) and ESTHERs (1). In contrast, the genomes of Lokiarchaeota encoded for most CAZymes and ESTHERs (~80 and ~40, respectively) and Heimdall- and Thorarchaeota for most of the peptidases (~35). However, the potential to degrade complex substrates is similar among the different Asgard archaea, when compared to their overall proteome size (Suppl. Figure 4). Notably, the main difference is the relative low number of predicted esterases in *Odinarchaeum*, which is in agreement with the lack of β-oxidation genes encoded in its genome. Potential substrates for these enzymes include complex carbohydrates, such as starch and glycogen (GH13, GH57, GH133), cellulose (GH12, GH5) or arabinan (GH93). Additionally, β-galactosidases (GH2), β-glucosidases (GH3) and α-mannosidases (GH38) might be involved in the degradation of oligosaccharides. A subset of these CAZymes were predicted to be extracellular, suggesting the degradation of more complex carbohydrates outside of and subsequent uptake into the cell. For example, genomes of Heimdallarchaeota and Lokiarchaeota encode for potentially secreted α-amylases (GH57 detected in AB125, LC3 and GC14_75) that cleave sugars from starch[25]. Consistent with this finding, we detected carbohydrate transporters in their genomes, including a potential disaccharide transport system in Heimdallarchaeota and Lokiarchaeota (transporter classification database (TCDB) ID: 3.A.1.1.22, 3.A.1.1.30, respectively) that could import sugars cleaved by secreted α-amylases (Suppl. Table 3). This observation as well as the presence of genes for most of the glycolytic pathway in Asgard genomes suggests that these genomes are capable to transform more complex carbohydrates and simple sugars to acetyl-CoA.

Aside from carbohydrate-degradation, genomes of Asgard archaea encode for several peptidase families (Suppl. Table 4). Few of these peptidases are predicted to be secreted and those mostly belong to the alkaline serine peptidase family S08 (detected in most of the genomes, Suppl. Table 4), which is implicated in nutritional substrate degradation[26]. In agreement with this, we detected several peptide transport systems across Asgard genomes. These include oligopeptide (Opp, TCDB IDs 3.A.1.5.12, 3.A.1.5.15 and 3.A.1.5.29) and dipeptide transport systems (Dpp, TCDB ID 3.A.1.5.39) in most of the Asgard genomes. Notably, oligopeptide transporters of the Opp/Dpp family can also be involved in complex carbohydrate transport, such as transport of mannans, rhamnose or xylan in *Thermotoga maritima*[27]. While genes for the degradation of rhamnose or xylans were absent, we frequently detected genes encoding α-mannosidases (GH38) and Opp transporters in the same genomes but not genetically linked on the same contig (*Lokiarchaeum* CR_4, *Thorarchaeum* AB_25, *Thorarchaeum* SMTZ-45 and SMTZ1-45). Additionally, we detected several uptake mechanisms for amino acids, including the amino acid permease YhdG/CtrA (TCDB ID 2.A.3.6.1) in all genomes except *Odinarchae*um, a transport system for branched chain amino acid in Thorarchaeota and Heimdallarchaeota (TCDB IDs 3.A.1.4.1 and 3.A.1.4.10) and basic amino acids in Thorarchaeota (TCDB ID 3.A.1.3.27). Most genomes of Asgard members encode genes involved in the intracellular degradation of peptides include potential oligopeptidases (M03, M13, S09), dipeptidases (M19, M38, S51, T02), aminopeptidases (M24, M29, M42, S33) and carboxypeptidases (M20, M32, S12) (Suppl. Table 4). Our analyses indicate that the key genes encoding proteins for the degradation of various amino acids (e.g. glutamate, alanine, glycine etc.) seem to be present in all lineages (Suppl.Tables 1 and 2). Amino acid degradation products such as pyruvate and oxoglutarate can then enter the TCA and contribute to the generation of reducing equivalents. Finally, the genomes of *Odinarchaeum* as well as Lokiarchaeota encode a complete suite of enzymes of the urea cycle, which may tie into the arginine metabolism (Suppl. Tables 1 and 2).

Consistent with the presence of fatty acid degradation genes in most genomes, we also find several genes that for example code for proteins belonging to the hydrolase family 4, which includes the monoglyceride lipase/lysophospholipase subfamily (Suppl. Table 4). Members of this subfamily have a broad substrate range but generally degrade monoacylglycerides to free fatty acids, which could subsequently be fed into the β-oxidation pathway. Consistent with the absence of this pathway in *Odinarchae*um, we did not detect any potential lipases in this genome. Apart from lipid degradation, most genomes except *Odinarchaeum* also encode for haloalkane dehydrogenases, members of the carbohydrate esterase CE10 family (i.e. para-nitrobenzyl esterases) and the lipase family XIII, which can act on acyl chain esters of butyrate or valerate[28].

Fatty acids (FA). One of the characteristics that distinguish archaeal lipids from those of bacteria and eukaryotes is the presence of isoprenoid and not fatty acyl chains[29]. Over the past three decades, a few notable exceptions to this observation have been reported in the Halobacteria[30,31]. Indeed, surveys of archaeal genomes revealed components of both fatty acid synthesis and breakdown[32,33]. In eukaryotes and bacteria, fatty acids are synthesized or oxidized on two different carrier molecules, acyl-carrier protein (ACP) or CoA respectively. However, in most archaea, fatty

acids are likely synthesized and oxidized on CoA[33,34]. While the genomes of all members of the Asgard archaea encode canonical enzymes to synthesize archaeal lipids (with the exception of the lack of genes encoding glycerol-1-phosphate dehydrogenase in Lokiarchaeota (Fig. 1, Suppl. Figure 2)), we identified multiple homologues of fatty acid metabolism proteins in each of the Asgard genomes except Odinarchaeota. This suggests that most of the Asgard archaea are capable of fatty acid degradation and synthesis. Here, we describe the pathway with respect to fatty acid breakdown although we suspect this pathway could also function in fatty acid synthesis, which has been reported elsewhere[32,33] (Suppl. Figure 2).

Long chain fatty acid CoA ligase - COG0318. Fatty acids destined for degradation are first activated with CoA via long chain fatty acid CoA ligase (COG0318) to generate an acyl-CoA. This protein family includes a variety of CoA ligases (e.g., Acyl-CoA synthetase, 2-succinylbenzoate--CoA ligase, medium and long chain fatty acid CoA ligase). With the exception of Odinarchaeota, each of the Asgard genomes encode multiple paralogues of this protein (Suppl. Table 1 and 2). To determine if any of these paralogues could be involved in fatty acid metabolism, we reconstructed the evolutionary history of this protein using sequences retrieved with BLAST against the nr and swissprot databases (see Methods for details, Suppl. Figure 5). We observed that the proteins are distributed across prokaryotic and eukaryotic diversity in multiple paralogues, though poor backbone support makes it difficult to determine the exact function of these proteins. Interestingly, *Heimdallarchaeum* LC2 has a MenE-like homologue (OLS23766) that might be involved in quinone metabolism (discussed below).

Acyl-CoA dehydrogenase (ACAD) COG1960. The resulting acyl-CoA can be oxidized via either an acyl-CoA dehydrogenase (ACAD, COG1960) or 4-hydroxybutyryl-CoA dehydratase (COG2368) to generate an acyl-2-enoyl-CoA. Most organisms have multiple paralogues of ACAD enzymes that are specific for different chain-lengths of fatty acids[35]. We observed multiple copies of COG1960 in each of the non-Odinarchaeota Asgards suggesting these organisms might be capable of metabolizing fatty acids (Suppl. Table 5). To help determine the substrate of the various Asgard ACADs, we performed a large phylogenetic analysis of ACADs across the tree of life with an emphasis on those sequences where the substrate specificity is known as previously reported in[35] (Suppl. Figure 6). Since these gene families consisted of 1000s of members, we subdivided the dataset into three main clades based on a preliminary phylogenetic analysis (see Methods for details). When possible, sub-clade distinctions were made based on representative sequences reported in[35]. The number of distinct paralogues identified in each Asgard genome ranged from 1-6 as indicated by numbers within the circles on Suppl. Figure 2b. Clade 1 (Suppl. Figure 6a) consists of two unclassified clades (clade 1a and 1b) with sequences from *Lokiarchaeum* CR4 and all the Thorarcheota and a sub-clade of medium chain acyl-CoA dehydrogenases (clade 1c; Suppl. Figure 6a). Within clade 2, *Heimdallarchaeum* LC2 and LC3 resolved in a clade sister to eukaryotic and bacterial ACAD10/11 sequences (Suppl. Figure 6b). The ACAD10 and 11 proteins in humans have been linked to branched chain (16C) and long-chain (20-26C) metabolism respectively[36], although the function of these ACADs remains largely unknown in other organisms. The Asgards

branch throughout the rest of clade 2, with the majority grouping with other archaeal sequences in the unclassified clade 2c and clade 2d (Suppl. Figure 6b). Clade 3 consists of mostly short chain (clade 3a and 3b) or branched chain (clade 3b and 3e) dehydrogenases (Suppl. Figure 6c). These clade 3 dehydrogenases were found only in the Lokiarchaeota and Heimdallarchaeota genomes but not in Thorarchaeota.

In general, the poor resolution of the tree and patchy distribution of the ACAD genes across the Asgards and Archaea makes it challenging to infer the evolutionary history of these proteins. Some Asgard ACAD sequences represent clear cases of recent events of horizontal gene transfer (HGT) from bacteria to archaea (e.g., Heimdallarchaeota OLS19783 and OLS26460, sub-clade 2a; Heimdallarchaeota OLS24605 sub-clade 2e; Heimdallarchaeota in sub-clade 3c, Heimdallarchaeota OLS26526 in sub-clade 3d; Suppl. Figure 6) while other proteins are found throughout archaea (e.g., sub-clades 2c and 2d), suggesting they could be conserved feature of the Asgards or HGTs from other archaea. The lack of studied representatives within many of the ACAD clades makes it difficult to predict the function of the Asgard sequences. However, we suspect that at least Lokiarchaeota and Heimdallarchaeota are capable of metabolizing short branched and unbranched acyl-CoA chains because they have homologues of clade 3a and 3b enzymes (Suppl. Figure 6c). Despite the absence of well-characterized bacterial or eukaryotic ACAD genes in archaea (e.g., medium chain ACAD, clade 1c; very long chain ACAD, clade 2a), *Archaeoglobus fulgidus* is able to degrade long-chain fatty acids[37]. This suggests that there might be alternative paralogues that archaea use to metabolize fatty acids that are distinct from their bacterial and eukaryotic counterparts. Prime candidates for such paralogues could be those sequences found in clade 2c or 2d that are enriched in archaeal representatives.

ACAD alternative - aromatic ring hydroxylase (ARH) or 4-hydroxybutyryl-CoA dehydrogenase - COG2368. Dibrova and colleagues[33] recognized that ARH represents an analogue of the ACAD enzymes and only appeared in archaeal genomes with other fatty acid metabolism genes. This prediction is supported by previous studies that demonstrated that ARH has ACAD-like activity in *Clostridium*[38] suggesting that ARH could replace ACAD in fatty acid biosynthesis. We analyzed the evolutionary history of this protein across the tree of life and found that, in general, this gene is rare in archaea (Suppl. Figure 7). Many of the archaeal sequences, including those encoded by genomes of Loki- and Thorarchaeota, cluster together in a divergent clade composed of Cren- and Euryarchaeota suggesting these archaeal paralogues could share a common origin. However, the remainder of the Asgard sequences group mostly with bacteria, suggesting these sequences derive from bacteria-Asgard HGT events.

Enoyl-CoA hydratase - ECH - COG1024. The acyl-2-enoyl-CoA produced by ACAD or the ACAD alternative enzymes discussed above is subsequently hydrated to 3-hydroxyacyl-CoA by the action of enoyl-CoA hydratase (ECH; COG1024). We observed many copies of COG1024 in the Loki-, Thor- and Heimdallarchaeota genomes, and as many as 23 copies in Lokiarchaeum (Suppl. Table 5). Of these 23 Lokiarchaeum ECH homologues, seven were excluded as they were very similar to another copy (due to strain heterogeneity[39]) or too short for further analysis. Like ACAD,

ECH are part of a large superfamily. To refine our inferences, we therefore split the dataset into two distinct clades, ECH1 and ECH2 (Suppl. Figure 8 and 9). In general, support along the backbone of both clade 1 and clade 2 phylogenies is poor. We observed that this gene is present in multiple paralogous copies across prokaryotes and eukaryotes. Each non-Odinarchaeota Asgard genome encoded at least 1 paralogue of ECH as indicated by numbers within the circles on Suppl. Figure 2b. As previously suggested by Dibrova and colleagues, the origin of this gene in Archaea is best explained by multiple independent HGT events from bacteria. For example, Asgard sequences that branch within a clade of only bacteria rather than grouping with sequences of other members of the Asgard archaea likely represent more recent transfer events (e.g., clade 1, OLS26255 *Heimdallarchaeum* LC 3; clade 2, KKK42140, OLS14134, KKK40657, Lokiarchaeota).

3-hydroxyacyl-CoA dehydrogenase - HDH - COG1250. The 3-hydroxyacyl-CoA generated by ECH is oxidized further by 3-hydroxyacyl-CoA dehydrogenase (HDH; COG1250) to generate 3-ketoacyl-CoA. We observed that most of the non-Odinarchaeota Asgards have at least one copy of this gene with Lokiarchaeota having as many as eight copies. Phylogenetic analyses revealed that there are multiple paralogues of this gene across Asgards as indicated by numbers within the circles in Suppl. Figure 2b. Most of the Asgard sequences branch with other archaea suggesting that these proteins could have an archaeal origin (Suppl. Figure 10). However, some of the Lokiarchaeota sequences branch with bacteria (e.g., KKK40272, KKK40637, KKK42255, and KKK41074) and thus could have been acquired via HGT events.

β*-ketothiolase - acetoacetyl-CoA acyltransferase - BKL/AACT - COG0183.* The final step of β-oxidation is catalyzed by β-ketothiolase (BKL, COG0183) which cleaves the 3-ketoacyl-CoA to form acetyl-CoA and an acyl-CoA molecule that is two carbons shorter. This family of enzymes includes the acetoacetyl-CoA transferase (AACT) enzymes which catalyze acetoacetyl-CoA formation from acetyl-CoA as the first step in the mevalonate pathway for the biosynthesis of isoprenoids in archaea. All of the Asgard genomes (except *Heimdallarchaeum* AB125) have at least one copy of BKL/AACT. Initial phylogenetic analysis of this superfamily of proteins revealed two distinct clades of sequences composed of mainly archaea (clade 1; Suppl. Figure 11) or bacteria (clade 2; Suppl. Figure 12). For ease of discussion, we labeled the subclades of clade 1 A-M however the corresponding clade identifiers first described by Dibrova et al. can be found in Suppl. Table 5. The Asgard sequences branch throughout clade 1 with other archaea. In general, the tree topology does not reflect a vertical inheritance pattern for many of the Asgard sequences. In fact, there are no clades that have a representative sequence from each of the Asgard phyla (i.e., Loki-, Thor-, Heimdall- and Odinarchaeota), suggesting that these genes have either been subject to multiple replacements via HGT or were differentially lost among the different Asgard phyla. Within clade 2, many of the Asgard homologues branch with bacteria (e.g., *Heimdallarchaeum* LC3 OLS23724; *Lokiarchaeum* CR4 OLS15559, OLS12682, OLS15498, OLS14603), suggesting they might derive from bacteria-Asgard HGT events. However, at least one clade includes seven representative sequences from Loki-, Thor-, and Heimdallarchaeota phyla (Suppl. Figure 11, bottom clade contains

Heimdallarchaeum LC3 sequence OLS26180) and branches with other archaea, and could therefore represent an ancient feature of the Asgard superphylum.

According to previous studies, some of the archaeal BKL/AACT sequences found in clade 1 (subclades 1B, 1C, 1D and 1H) are encoded next to genes related to mevalonate metabolism[33]. To expand on this observation, we searched the 15 genes upstream and downstream of the Asgard BKL/AACT for genes related to β-oxidation (COGs 0318, 1960, 2368, 1024, 1042 or 1250) and mevalonate metabolism (COG3425) (Suppl. Figure 13). We found that some of the Asgard BKL/AACT sequences in subclades 1A, 1D, 1H, 1J, 1K, and 1L are linked to β-oxidation associated genes while those in 1B, 1E, and 1L are linked to mevalonate associated genes (e.g., HMG-CoA synthase). Within clade 2, only two of the Lokiarchaeota sequences appear to be linked to β-oxidation genes (Suppl. Figure 12). The gene proximity of the BKL/AACT sequences to various elements of β-oxidation and mevalonate metabolism could be used as a proxy for determining in which pathway these proteins participate, although further functional characterization is needed.

A note on fatty acid biosynthesis. Bacteria and eukaryotes typically have different enzymes dedicated to β-oxidation and biosynthesis of fatty acids. For example, the steps catalyzed by ACAD and HDH are in fact catalyzed by members of the short-chain dehydrogenase protein family (COG1028) namely enoyl-ACP reductase and ketoacyl-ACP reductase. We detected over 150 genes within this protein family across the Asgard superphylum, some of which might be dedicated for fatty acid metabolism, however, these pathways have yet to be characterized in archaea (Suppl. Table 5). Another fundamental difference between β-oxidation and fatty acid biosynthesis is the use of CoA versus acyl-carrier protein (ACP). In general, ACPs are rare in archaea and likely represent a bacterial feature[33,34]. Notably, however, we identified homologues of ACP in *Heimdallarchaeum* LC3 and all members of Thorarchaeota (Suppl. Table 5), suggesting that these organisms might be capable of ACP-mediated fatty acid biosynthesis. In the other Asgards and archaea without ACPs, it is possible that the β-oxidation enzymes might be able to synthesize fatty acids using CoA as the carrier molecule as is the presumed mechanism in other archaea[33,34]. Indeed, recent studies using synthetic biology, have successfully engineered the β-oxidation pathways of *E. coli* and yeast to elongate fatty acids[40,41] suggesting that these pathways have the potential to function in both directions.

Hydrocarbons. Notably, all analyzed Loki- and Thorarchaeota as well as *Heimdallarchaeum* AB125 contain several genes coding for pyruvate formate lyase (Pfl) domain (IPR004184) proteins (Suppl. Tables 1 and 2). This protein family includes glycyl radical enzymes, some of which are involved in the anaerobic activation of hydrocarbons through the addition of fumarate[42]. The glycyl is activated by glycyl-activating enzymes (reviewed in[43]), the genes for which are present in all Asgard archaea and occur in a gene cluster with IPR004184-domain containing proteins in *Lokiarchaeum* CR4 and *Heimdallarchaeum* AB125. Our phylogenetic analyses of the Pfl domain proteins show that archaeal homologues including those of Asgard archaea do not represent *bona fide* Pfl (Suppl. Figure 14). In contrast, they affiliate with those proteins comprising known alkylsuccinate and benzylsuccinate synthases[44], choline

trimethylamine lyases[45] or 4-hydroxyphenlyacetate decarboxylases[46], some of which allow the activation of hydrocarbons by fumarate addition. However, the different archaeal lineages comprise various separate clusters in phylogenetic analyses indicating independent gene transfers from different bacterial sources without clear affiliation to specific characterized enzymes. Thus, the function of these enzymes in Asgard archaea is unresolved. Yet, it seems possible, that at least some of these protein homologues could function in the activation of different hydrocarbons. For instance, a Pfl domain protein of *Archaeoglobus fulgidus* related to a homologue of *Thorarchaeum* SMTZ1_83 (Suppl. Figure 14: A0A135VWA9, arrow) has been analyzed previously and was suggested to represent an alkylsuccinate synthase involved in the activation of C16-alkanes by fumarate addition[37]. Furthermore, it was shown that *Thermococcus sibiricus* has the potential to grow on an alkane likely using its PFL-homologue (Suppl. Figure 14, C6A251, arrow). Prospective analyses are required to test the hypothesis of growth on hydrocarbons in the respective Asgard archaea and to elucidate the exact pathway of hydrocarbon degradation in archaea, which may differ from bacteria. For example, in bacteria, malonyl-CoA decarboxylase (IPR007956, IPR035372) is critical for the alkane degradation pathway[47], though we could not detect this protein in archaea. However, several other proteins involved in alkane degradation in bacteria[47] belong to enzyme families that also comprise proteins involved in the 3-hydroxypropionate/4-hydroxybutyrate carbon fixation pathway in some members of the TACK archaea. Candidate genes coding for enzymes of these protein families are present in the genomes of the different Asgard lineages (except for Odinarchaeota; Suppl. Tables 1 and 2) but also in several members of the Archaeoglobales, in which they were suggested to enable alkane degradation[17].

3) Electron transport chains differ among the Asgard lineages

[Ni-Fe]-hydrogenases. All members of the Asgards lack [FeFe]-hydrogenases or the methanogen-specific [Fe]-hydrogenases. However, all Asgard genomes encode various [NiFe]-hydrogenases, which were annotated based on classification of the large subunit using HydDB[48], phylogenetic analyses (Suppl. Table 2, Fig. 2) and operon architecture (Suppl. Figure 3). In particular, the Asgard genomes encode [NiFe]-hydrogenases belonging to Group 3 and Group 4, yet lack representatives of Group 1 and Group 2 [NiFe]-hydrogenases. First of all, both the genomes of Thorarchaeota, *Heimdallarchaeum* LC2 and LC3 as well as of *Lokiarchaeum* GC14_75 encode genes for [NiFe]-Hydrogenases belonging to Group 3c, which are located in gene clusters encoding all or some components of heterodisulfide reductases (Suppl. Figure 3). In methanogens, hydrogenase (MvhADG)-heterodisulfide reductase (HdrABC) complexes mediate electron bifurcation, with electrons from H_2 oxidation being simultaneously transferred to ferredoxin and heterodisulfide[49]. However, the substrate for these enzymes outside the methanogens (which use CoM-S-S-CoB) remains to be determined. While, the Heimdallarchaeota (LC2 and LC3) large subunit 3c homologues have retained the C-XX-C motifs at the C-terminus, this motif is not conserved in most of the thor- and lokiarchaeal homologues. It thus needs to be confirmed that these Group 3c [NiFe]-hydrogenases can bind the [NiFe] centers required to mediate H_2 oxidation[49]. In addition, Loki-, Odin- and Thorarchaeota as well as *Heimdallarchaeum*

LC3 contain gene clusters encoding [NiFe]-hydrogenases belonging to Group 3b (Suppl. Figure 3), which are bidirectional and may either evolve H_2 using electrons from NADPH or recycle H_2 to produce NADPH as reported for members of the Thermococcales[50,51]. While, the Group 3b enzyme complexes of *Pyrococcus furiosus* were shown to also have sulfhydrogenase activity (i.e. to reduce elemental sulfur to H_2S) *in vitro*[52], this does not seem to be their physiological function ([51] and references therein).

Finally, genomes of Heimdall- and Odinarchaeota also encode various membrane-bound Group 4 [NiFe]-hydrogenases, which are only distantly related to known Group 4 subgroups. In fact, the addition of homologues from novel archaeal genomes to our phylogenetic analyses, revealed that Group 4 hydrogenases are even more diverse than anticipated earlier[53] and suggests that future efforts are needed to define novel subgroups. Currently, most of these archaeal Group 4 large subunit homologues, including those present in Asgard archaea, comprise novel clusters within the loosely defined respiratory H_2-evolving 4g subgroup (Fig. 2). While, the exact function is unconfirmed, it has been suggested that the previously described Group 4g hydrogenases can couple ferredoxin oxidation to proton reduction in a simple electron chain that can contribute to the membrane potential and enhance overall energy yield. In order to get more insights into the potential function of group 4 [NiFe]-hydrogenases of Asgard archaea, we investigated the arrangement of the corresponding gene clusters. This revealed that the arrangement of their gene clusters (Suppl. Figure 3) is highly variable, in agreement with the large sequence diversity of the key subunit of these Group 4 [NiFe]-hydrogenases. However, all group 4 [NiFe]-hydrogenases seem to be membrane-anchored and ferredoxin represents the most likely co-substrate. Furthermore, the gene cluster architecture suggests, that at least two Group 4 hydrogenases of Odinarchaeum (OdinLCB4_14620, OdinLCB4_02560) and the Group 4 hydrogenase of *Heimdallarchaeum* LC2 (HeimC2_23020) can mediate sodium/proton translocation similar to *Pyrococcus furiosus* [54] as indicated by the presence of NuoL-like (also Mrp antiporter-like) membrane subunits (Suppl. Figure 3). Currently, the gene cluster that encodes the group 4 [NiFe]-hydrogenase of *Heimdallarchaeum* AB125 does not include genes encoding NuoL-like subunits (Suppl. Figure 3). However, in this regard, it has to be noted that the contig on which this gene cluster is located starts with the hypD gene (OLS33135). Furthermore, *nuoL/M/N-like* genes (e.g. OLS33159, OLS33160, OLS29628) are encoded towards the end of two other genomic contigs of this organism. This indicates that the gene cluster displayed in Suppl. Figure 3 is currently incomplete as a result of genome assembly that has split the hydrogenase gene cluster into separate contigs. Thus and based on the similarity to the large subunit of the Group 4 Hydrogenases of *Heimdallarchaeum* LC2 (Figure 2), it is most likely that the Group 4 hydrogenase of *Heimdallarchaeum* AB125 is also ion conductive and thus involved in energy conservation.

Complex I and alternative NADH:quinone reductases. Only genomes of Heimdallarchaeota and Thorarchaeota seem to encode a multisubunit NADH dehydrogenase (Complex 1) (Suppl. Table S2) including a homolog of NuoD (Fig. 2). However, candidates for an alternative NADH:quinone reductase are present in Loki- and Thorarchaeota. Genomes of members of these phyla encode several proteins with nitronate monooxygenase

domains (PF03060). It was recently reported that this protein family includes a new class of NADH:quinone reductases (PA1024)[55]. Interestingly, at least one PF03060 domain protein of each Loki- and Thorarchaeota is much more similar to the NADH:quinone reductases of *Pseudomonas aeruginosa* PAO1 (PA1024) (ca. 40% AA identity) than to its nitronate monooxygenase (PA4202) (ca. 28% AA identity). This may suggest that PF03060 domain proteins in these Asgard archaea may represent novel types of quinone reductases and could comprise a NADH:quinone reductases, which could for example function in the re-oxidation of NAD(P)H generated during growth on organic substrates.

Reductive dehalogenases. Surprisingly, genomes of all Asgard archaea except for *Odinarchaeum* encode various proteins assigned to epoxyqueuosine reductases (COG01600), some of which have significant similarity to reductive dehalogenase domains (IPR028894) (Suppl. Table 2). In bacteria, reductive dehalogenases serve as terminal reductases enabling the degradation of organohalides[56] using H_2, different organic substrates (e.g. pyruvate and acetate) or even NADPH as electron donors[57]. Organohalides such as halogenated phenols, dioxins, biphenyls, and aliphatic hydrocarbons represent persistent environmental pollutants and bacteria able to engage in dehalogenation of these compounds are of great ecological importance. Reductive dehalogenases are corrinoid Fe-S containing proteins and homologous to epoxyqueuosine reductases (COG01600)[58]. Notably, our phylogenetic analyses of this protein family using a previously described backbone dataset[59] revealed that genomes of Loki-, Thor- and *Heimdallarchaeum* LC2 and LC3 as well as Theionarchaea each encode at least one putative *bona fide* reductive dehalogenase (Suppl. Figure 15, dark green) suggesting the ability to use organohalides as terminal electron acceptors. The function of other homologs belonging to the epoxyqueuosine reductase family and which lack IPR domains of canonical reductive dehalogenases (Suppl. Figure 15, light green box)[58] is currently unclear, yet it may be speculated that some could represent novel electron acceptors with yet unknown the substrates.

In organohalide-respiring bacteria, the reductive dehalogenase genes are generally encoded in an operon with a gene encoding a membrane anchoring protein. However, since homologues of these membrane anchors could not be detected in the Asgard archaea, it is difficult to determine if these reductive dehalogenases are membrane-associated or soluble enzymes. Therefore, it will be important to characterize some of these proteins biochemically to determine whether Asgard archaea can indeed engage in the degradation of specific pollutants and elucidate the substrate spectrum of these proteins. For example, in Loki- and Thorarchaeota, which appear to lack classical terminal reductases, these reductive dehalogenases could allow the re-oxidation of the quinols generated during β-oxidation and ETF.

Terminal oxidase and nitrate reductase in Heimdallarchaeota. Surprisingly, genomes of *Heimdallarchaeote* LC2 and LC3 encode terminal A-type heme-copper oxidases (Suppl. Figure 16a), which may allow the respective organisms to use oxygen as terminal electron acceptor. Furthermore, under anoxic conditions, the presence of a respiratory nitrate reductase (Suppl. Table 1) seems to enable the use of nitrate as terminal acceptor through anaerobic

phosphorylation. Notably, a closer investigation of the alpha subunits of the nitrate reductase (NarG) encoded by *Heimdallarchaeum* LC2 and LC3 genomes, revealed that they belong to the bacterial-type nitrate reductase family (IPR006468) and lack the TAT signal motif common in canonical archaeal-type nitrate reductases which are localized at the extracellular site of the cytoplasmic membrane. Thus, Nar of Heimdallarchaeota is likely located in the cytoplasm similar to the bacterial-type Nar[60-62]. Phylogenetic analyses of NarG revealed that the Heimdallarchaeota homologues form a monophyletic cluster with the bacterial-type nitrate reductase of *Methanoperedens* sp. BLZ1 (Suppl. Figure 16b) as well as with a homologue of *Methylomirabilis oxyfera*, *Nitrolancea hollandica*, *Nitrococcus mobilis* and a *Nitrobacter* sp. species. Most likely, the few archaeal genomes that encode a bacterial version of Nar (Suppl. Figure 16b) have acquired the corresponding genes independently from bacterial sources.

Other potential electron chain components. Besides the presence of terminal reductases and a Complex I in *Heimdallarchaeum* LC2 and LC3, the genomes of these organisms encode a membrane-bound succinate dehydrogenase/fumarate reductase (Complex II), as well as a putative electron transfer flavoprotein quinone:oxidoreductase complex (ETF-QO; composed of FixA, FixB, FixC and FixX), both of which may allow the reduction of quinone-species (Fig. 1; Suppl. Tables 1 and 2). While genomes of Loki- and Thorarchaeota also encode FixA and FixB homologues as well as candidate proteins for FixC (belonging to arCOG00570), the latter did not occur in a gene cluster with FixX homologues. It remains therefore unclear whether Loki- and Thorarchaeota have a complete membrane-associated ETF-QO. In this regard, it is notable that genomes of Loki- and Thorarchaeota encode a large amounts of homologues belonging to subunits of soluble heterodisulfide reductases comprised of HdrA, HdrB and HdrC as well as of the D subunit of membrane-bound heterodisulfide reductases (which also includes HdrE)[9]. However, similar to *Methanomassiliicoccales*[63], genomes of Loki- and Thorarchaeota do not seem to encode homologues of HdrE, and the functional role of their HdrD homologues remains to be determined. For example, some of the loki- and thorarchaeal HdrD family homologues (arCOC00333) may be involved in the re-oxidation of quinol species generated by ETF during growth on organic substrates (e.g. β-oxidation) (Fig. 1). It also remains to be determined whether the succinate dehydrogenases/fumarate reductases of Loki- and Thorarchaeota are membrane-associated and could represent another means for the re-oxidation of quinol species (Fig. 1). Furthermore, genomes of most Asgard archaea, except for *Odinarchaeoum*, encode putative multihaem cytochromes (IPR011031) and/or cytochrome c-552/DMSO reductase-like, haem-binding domains (IPR019020), yet it is unclear whether these proteins play a role in electron transfer in these organisms. In two Thorarchaeota, the multihaeme cytochromes encode additional signature domains for cytochrome c552 (IPR003321), which occurs in formate-dependent cytochrome C nitrite reductases and catalyzes the reduction of nitrite to ammonia (Suppl. Tables 1, and 2)[64]. It remains to be investigated whether these thorarchaeal proteins, which are only distantly related to known nitrite reductases, could have similar functions. Most notably, *Heimdallarchaeum* LC2 and LC3 genomes code for cytochrome b561 domain proteins as well as a multitude of cupredoxin domain proteins, the latter of which may

represent important electron carriers (besides quinones) in these organisms and may shuttle reducing equivalents to their terminal oxidases (Fig. 1, Suppl. Table 2).

Menaquinone biosynthesis. All Asgard archaea genomes contain several genes encoding proteins potentially involved in ubiquinone/menaquinone biosynthesis. The set of genes is most complete for Heimdallarchaeota, supporting the idea that quinone species are components of their electron chains (Suppl. Table 1, Fig. 1). However, *Heimdallarchaeum* LC2 is the only representative of the Asgard archaea whose genome encodes homologues for most enzymes of the menaquinone biosynthesis pathway (Suppl. Tables 1 and 2; including MenB, MenF, MenD, MenE and candidates for MenA and MenG). For example, one of the steps is catalyzed by a member of the acyl-CoA synthetase (AMP-forming)/AMP-acid ligase II family. While genomes of all Asgard archaea encode representatives of this enzyme family (mainly functioning in β-oxidation), the *Heimdallarchaeum* LC2 genome uniquely encodes a homologue, which branches within the MenE clade in phylogenetic analyses and is annotated as a 2-succinylbenzoate-CoA ligase (Suppl. Figure 5). In contrast, the biosynthesis of menaquinones is less clear in *Heimdallarchaeum* LC3 and AB125. While they lack homologues of most canonical menaquinone biosynthesis genes, these genomes encode a homologue of MqnC, an enzyme of an alternative menaquinone biosynthesis pathway[65]. However, even though some of the genes annotated as ubiquinone biosynthesis genes may function in this alternative pathway, *Heimdallarchaeum* LC3 and AB125 seem to lack some enzymes characteristic of this pathway and the exact steps leading to menaquinone are therefore unclear in these latter organisms. Genomes of Loki- and Thorarchaeota encode only few candidate proteins for the biosynthesis of quinone species and the presence of quinones in these organisms needs to be investigated in future studies.

B. References

1 Zhang, Y., Zagnitko, O., Rodionova, I., Osterman, A. & Godzik, A. The FGGY carbohydrate kinase family: insights into the evolution of functional specificities. *PLoS Comput Biol* **7**, e1002318-e1002318, doi:10.1371/journal.pcbi.1002318
10.1371/journal.pcbi.1002318. Epub 2011 Dec 22. (2011).

2 Say, R. F. & Fuchs, G. Fructose 1,6-bisphosphate aldolase/phosphatase may be an ancestral gluconeogenic enzyme. *Nature* **464**, 1077-1081, doi:10.1038/nature08884
10.1038/nature08884. Epub 2010 Mar 28. (2010).

3 Brasen, C., Esser, D., Rauch, B. & Siebers, B. Carbohydrate metabolism in Archaea: current insights into unusual enzymes and pathways and their regulation. *Microbiology and Molecular Biology Reviews* **78**, 89-175, doi:10.1128/MMBR.00041-13
10.1128/MMBR.00041-13. (2014).

4 Sousa, F. L., Neukirchen, S., Allen, J. F., Lane, N. & Martin, W. F. Lokiarchaeon is hydrogen dependent. *Nature Microbiology* **1**, doi:Artn 16034 10.1038/Nmicrobiol.2016.34 (2016).

5 Seitz, K. W., Lazar, C. S., Hinrichs, K. U., Teske, A. P. & Baker, B. J. Genomic reconstruction of a novel, deeply branched sediment archaeal phylum with pathways for acetogenesis and sulfur reduction. *The ISME Journal*, doi:10.1038/ismej.2015.233 (2016).

6 Liu, Y. *et al.* Comparative genomic inference suggests mixotrophic lifestyle for Thorarchaeota. *ISME J* **12**, 1021-1031, doi:10.1038/s41396-018-0060-x (2018).

7 Ragsdale, S. W. & Pierce, E. Acetogenesis and the Wood-Ljungdahl pathway of CO(2) fixation. *Biochim Biophys Acta* **1784**, 1873-1898, doi:10.1016/j.bbapap.2008.08.012 (2008).

8 Adam, P. S., Borrel, G. & Gribaldo, S. Evolutionary history of carbon monoxide dehydrogenase/acetyl-CoA synthase, one of the oldest enzymatic complexes. *Proceedings of the National Academy of Sciences of the United States of America* **115**, E1166-E1173, doi:10.1073/pnas.1716667115
10.1073/pnas.1716667115. Epub 2018 Jan 22. (2018).

9 Thauer, R. K., Kaster, A. K., Seedorf, H., Buckel, W. & Hedderich, R. Methanogenic archaea: ecologically relevant differences in energy conservation. *Nat Rev Microbiol* **6**, 579-591, doi:10.1038/nrmicro1931
10.1038/nrmicro1931. Epub 2008 Jun 30. (2008).

10 Schuchmann, K. & Muller, V. Energetics and application of heterotrophy in acetogenic bacteria. *Appl Environ Microbiol*, doi:10.1128/AEM.00882-16 (2016).

11 Borrel, G., Adam, P. S. & Gribaldo, S. Methanogenesis and the Wood-Ljungdahl Pathway: An Ancient, Versatile, and Fragile Association. *Genome Biol Evol* **8**, 1706-1711, doi:10.1093/gbe/evw114 (2016).

12 Krzycki, J. A. Function of genetically encoded pyrrolysine in corrinoid-dependent methylamine methyltransferases. *Curr Opin Chem Biol* **8**, 484-491, doi:10.1016/j.cbpa.2004.08.012
10.1016/j.cbpa.2004.08.012. (2004).

13 Ticak, T., Kountz, D. J., Girosky, K. E., Krzycki, J. A. & Ferguson Jr, D. J. A nonpyrrolysine member of the widely distributed trimethylamine methyltransferase family is a glycine betaine methyltransferase. *Proceedings of the National Academy of Sciences of the United States of America* **111**, E4668-4676, doi:10.1073/pnas.1409642111
10.1073/pnas.1409642111. Epub 2014 Oct 13. (2014).

14 Wang, S., Chen, Y., Cao, Q. & Lou, H. Long-Lasting Gene Conversion Shapes the Convergent Evolution of the Critical Methanogenesis Genes. *G3 (Bethesda)* **5**, 2475-2486, doi:10.1534/g3.115.020180
10.1534/g3.115.020180. (2015).

15 Hippler, B. & Thauer, R. K. The energy conserving methyltetrahydromethanopterin:coenzyme M methyltransferase complex from methanogenic archaea: function of the subunit MtrH. *FEBS Lett* **449**, 165-168 (1999).
16 Harms, U. & Thauer, R. K. Identification of the active site histidine in the corrinoid protein MtrA of the energy-conserving methyltransferase complex from Methanobacterium thermoautotrophicum. *Eur J Biochem* **250**, 783-788 (1997).
17 Estelmann, S. *et al.* Carbon dioxide fixation in 'Archaeoglobus lithotrophicus': are there multiple autotrophic pathways? *Fems Microbiology Letters* **319**, 65-72, doi:10.1111/j.1574-6968.2011.02268.x
10.1111/j.1574-6968.2011.02268.x. Epub 2011 Apr 4. (2011).
18 Tabita, F. R., Satagopan, S., Hanson, T. E., Kreel, N. E. & Scott, S. S. Distinct form I, II, III, and IV Rubisco proteins from the three kingdoms of life provide clues about Rubisco evolution and structure/function relationships. *J Exp Bot* **59**, 1515-1524, doi:10.1093/jxb/erm361
10.1093/jxb/erm361. Epub 2008 Feb 16. (2008).
19 Solden, L., Lloyd, K. & Wrighton, K. The bright side of microbial dark matter: lessons learned from the uncultivated majority. *Curr Opin Microbiol* **31**, 217-226, doi:10.1016/j.mib.2016.04.020 (2016).
20 Sato, T., Atomi, H. & Imanaka, T. Archaeal type III RuBisCOs function in a pathway for AMP metabolism. *Science* **315**, 1003-1006, doi:10.1126/science.1135999
10.1126/science.1135999. (2007).
21 Kono, T. *et al.* A RuBisCO-mediated carbon metabolic pathway in methanogenic archaea. *Nat Commun* **8**, 14007-14007, doi:10.1038/ncomms14007
10.1038/ncomms14007. (2017).
22 Stams, A. J. & Plugge, C. M. Electron transfer in syntrophic communities of anaerobic bacteria and archaea. *Nat Rev Microbiol* **7**, 568-577, doi:10.1038/nrmicro2166 (2009).
23 Jorgensen, S. L. *et al.* Correlating microbial community profiles with geochemical data in highly stratified sediments from the Arctic Mid-Ocean Ridge. *Proceedings of the National Academy of Sciences of the United States of America* **109**, E2846-2855, doi:10.1073/pnas.1207574109 (2012).
24 Jorgensen, S. L., Thorseth, I. H., Pedersen, R. B., Baumberger, T. & Schleper, C. Quantitative and phylogenetic study of the Deep Sea Archaeal Group in sediments of the Arctic mid-ocean spreading ridge. *Front Microbiol* **4**, 299-299, doi:10.3389/fmicb.2013.00299 (2013).
25 Janecek, S. & Blesak, K. Sequence-structural features and evolutionary relationships of family GH57 alpha-amylases and their putative alpha-amylase-like homologues. *Protein J* **30**, 429-435, doi:10.1007/s10930-011-9348-7
10.1007/s10930-011-9348-7. (2011).
26 Rawlings, N. D., Barrett, A. J. & Finn, R. Twenty years of the MEROPS database of proteolytic enzymes, their substrates and inhibitors. *Nucleic Acids Research* **44**, D343-350, doi:10.1093/nar/gkv1118
10.1093/nar/gkv1118. Epub 2015 Nov 2. (2016).
27 Conners, S. B. *et al.* An expression-driven approach to the prediction of carbohydrate transport and utilization regulons in the hyperthermophilic bacterium Thermotoga maritima. *J Bacteriol* **187**, 7267-7282, doi:10.1128/JB.187.21.7267-7282.2005
10.1128/JB.187.21.7267-7282.2005. (2005).
28 Levisson, M., van der Oost, J. & Kengen, S. W. Characterization and structural modeling of a new type of thermostable esterase from Thermotoga maritima. *FEBS J* **274**, 2832-2842, doi:10.1111/j.1742-4658.2007.05817.x
10.1111/j.1742-4658.2007.05817.x. Epub 2007 Apr 27. (2007).

29 Koga, Y., Nishihara, M., Morii, H. & Akagawa-Matsushita, M. Ether polar lipids of methanogenic bacteria: structures, comparative aspects, and biosyntheses. *Microbiol Rev* **57**, 164-182 (1993).
30 Pugh, E. L., Wassef, M. K. & Kates, M. Inhibition of fatty acid synthetase in Halobacterium cutirubrum and Escherichia coli by high salt concentrations. *Canadian journal of biochemistry* **49**, 953-958 (1971).
31 Falb, M. *et al.* in *Extremophiles* (2008).
32 Lombard, J., López-García, P. & Moreira, D. The early evolution of lipid membranes and the three domains of life. *Nature Reviews Microbiology* **10**, 507-515, doi:10.1038/nrmicro2815 (2012).
33 Dibrova, D. V., Galperin, M. Y. & Mulkidjanian, A. Y. Phylogenomic reconstruction of archaeal fatty acid metabolism. *Environ Microbiol* **16**, 907-918, doi:10.1111/1462-2920.12359 (2014).
34 Lombard, J., López-García, P. & Moreira, D. An ACP-independent fatty acid synthesis pathway in archaea: Implications for the origin of phospholipids. *Molecular Biology and Evolution*, doi:10.1093/molbev/mss160 (2012).
35 Swigonova, Z., Mohsen, A. W. & Vockley, J. Acyl-CoA dehydrogenases: Dynamic history of protein family evolution. *J Mol Evol* **69**, 176-193, doi:10.1007/s00239-009-9263-0
10.1007/s00239-009-9263-0. Epub 2009 Jul 29. (2009).
36 He, M. *et al.* Identification and characterization of new long chain acyl-CoA dehydrogenases. *Mol Genet Metab* **102**, 418-429, doi:10.1016/j.ymgme.2010.12.005 (2011).
37 Khelifi, N. *et al.* Anaerobic oxidation of long-chain n-alkanes by the hyperthermophilic sulfate-reducing archaeon, Archaeoglobus fulgidus. *The ISME Journal* **8**, 2153-2166, doi:10.1038/ismej.2014.58
10.1038/ismej.2014.58. Epub 2014 Apr 24. (2014).
38 Müh, U., Çinkaya, I., Albracht, S. P. J. & Buckel, W. 4-Hydroxybutyryl-CoA dehydratase from Clostridium aminobutyricum: Characterization of FAD and iron-sulfur clusters involved in an overall non- redox reaction. *Biochemistry*, doi:10.1021/bi9601363 (1996).
39 Spang, A. *et al.* Complex archaea that bridge the gap between prokaryotes and eukaryotes. *Nature* **521**, 173-+, doi:10.1038/nature14447 (2015).
40 Clomburg, J. M., Vick, J. E., Blankschien, M. D., Rodríguez-Moyá, M. & Gonzalez, R. A synthetic biology approach to engineer a functional reversal of the β-oxidation cycle. *ACS Synthetic Biology*, doi:10.1021/sb3000782 (2012).
41 Lian, J. & Zhao, H. Reversal of the β-oxidation cycle in saccharomyces cerevisiae for production of fuels and chemicals. *ACS Synthetic Biology*, doi:10.1021/sb500243c (2015).
42 Callaghan, A. V. Enzymes involved in the anaerobic oxidation of n-alkanes: from methane to long-chain paraffins. *Front Microbiol* **4**, 89-89, doi:10.3389/fmicb.2013.00089
10.3389/fmicb.2013.00089. eCollection 2013. (2013).
43 Shisler, K. A. & Broderick, J. B. Glycyl radical activating enzymes: structure, mechanism, and substrate interactions. *Arch Biochem Biophys* **546**, 64-71, doi:10.1016/j.abb.2014.01.020
10.1016/j.abb.2014.01.020. Epub 2014 Jan 31. (2014).
44 Leuthner, B. *et al.* Biochemical and genetic characterization of benzylsuccinate synthase from Thauera aromatica: a new glycyl radical enzyme catalysing the first step in anaerobic toluene metabolism. *Mol Microbiol* **28**, 615-628 (1998).
45 Craciun, S. & Balskus, E. P. Microbial conversion of choline to trimethylamine requires a glycyl radical enzyme. *Proceedings of the National Academy of Sciences of the United States of America* **109**, 21307-21312, doi:10.1073/pnas.1215689109
10.1073/pnas.1215689109. Epub 2012 Nov 14. (2012).
46 Selmer, T. & Andrei, P. I. p-Hydroxyphenylacetate decarboxylase from Clostridium difficile. A novel glycyl radical enzyme catalysing the formation of p-cresol. *Eur J Biochem* **268**, 1363-1372 (2001).

47 Jarling, R. *et al.* Stereochemical investigations reveal the mechanism of the bacterial activation of n-alkanes without oxygen. *Angew Chem Int Ed Engl* **51**, 1334-1338, doi:10.1002/anie.201106055
10.1002/anie.201106055. Epub 2011 Nov 30. (2012).
48 Sondergaard, D., Pedersen, C. N. & Greening, C. HydDB: A web tool for hydrogenase classification and analysis. *Sci Rep* **6**, 34212-34212, doi:10.1038/srep34212
10.1038/srep34212. (2016).
49 Buckel, W. & Thauer, R. K. Energy conservation via electron bifurcating ferredoxin reduction and proton/Na(+) translocating ferredoxin oxidation. *Biochim Biophys Acta* **1827**, 94-113, doi:10.1016/j.bbabio.2012.07.002
10.1016/j.bbabio.2012.07.002. Epub 2012 Jul 16. (2013).
50 Kanai, T. *et al.* Distinct physiological roles of the three [NiFe]-hydrogenase orthologs in the hyperthermophilic archaeon Thermococcus kodakarensis. *J Bacteriol* **193**, 3109-3116, doi:10.1128/JB.01072-10
10.1128/JB.01072-10. Epub 2011 Apr 22. (2011).
51 Jenney Jr, F. E. & Adams, M. W. Hydrogenases of the model hyperthermophiles. *Ann N Y Acad Sci* **1125**, 252-266, doi:10.1196/annals.1419.013
10.1196/annals.1419.013. (2008).
52 Ma, K., Weiss, R. & Adams, M. W. Characterization of hydrogenase II from the hyperthermophilic archaeon Pyrococcus furiosus and assessment of its role in sulfur reduction. *J Bacteriol* **182**, 1864-1871 (2000).
53 Greening, C. *et al.* Genomic and metagenomic surveys of hydrogenase distribution indicate H2 is a widely utilised energy source for microbial growth and survival. *The ISME Journal* **10**, 761-777, doi:10.1038/ismej.2015.153
10.1038/ismej.2015.153. Epub 2015 Sep 25. (2016).
54 Yu, H. *et al.* Structure of an Ancient Respiratory System. *Cell* **173**, 1636-1649 e1616, doi:10.1016/j.cell.2018.03.071 (2018).
55 Ball, J., Salvi, F. & Gadda, G. Functional Annotation of a Presumed Nitronate Monoxygenase Reveals a New Class of NADH:Quinone Reductases. *J Biol Chem* **291**, 21160-21170, doi:10.1074/jbc.M116.739151
10.1074/jbc.M116.739151. Epub 2016 Aug 8. (2016).
56 Bommer, M. *et al.* Structural basis for organohalide respiration. *Science* **346**, 455-458, doi:10.1126/science.1258118
10.1126/science.1258118. Epub 2014 Oct 2. (2014).
57 Jugder, B. E., Ertan, H., Lee, M., Manefield, M. & Marquis, C. P. Reductive Dehalogenases Come of Age in Biological Destruction of Organohalides. *Trends Biotechnol* **33**, 595-610, doi:10.1016/j.tibtech.2015.07.004
10.1016/j.tibtech.2015.07.004. (2015).
58 Miles, Z. D., McCarty, R. M., Molnar, G. & Bandarian, V. Discovery of epoxyqueuosine (oQ) reductase reveals parallels between halorespiration and tRNA modification. *Proceedings of the National Academy of Sciences of the United States of America* **108**, 7368-7372, doi:10.1073/pnas.1018636108
10.1073/pnas.1018636108. Epub 2011 Apr 18. (2011).
59 Hug, L. A. *et al.* Overview of organohalide-respiring bacteria and a proposal for a classification system for reductive dehalogenases. *Philos Trans R Soc Lond B Biol Sci* **368**, 20120322-20120322, doi:10.1098/rstb.2012.0322
10.1098/rstb.2012.0322. Print 2013 Apr 19. (2013).

60 Arshad, A. *et al.* A Metagenomics-Based Metabolic Model of Nitrate-Dependent Anaerobic Oxidation of Methane by Methanoperedens-Like Archaea. *Front Microbiol* **6**, 1423-1423, doi:10.3389/fmicb.2015.01423
10.3389/fmicb.2015.01423. eCollection 2015. (2015).
61 Bertero, M. G. *et al.* Insights into the respiratory electron transfer pathway from the structure of nitrate reductase A. *Nat Struct Biol* **10**, 681-687, doi:10.1038/nsb969
10.1038/nsb969. Epub 2003 Aug 10. (2003).
62 Martinez-Espinosa, R. M. *et al.* Look on the positive side! The orientation, identification and bioenergetics of 'Archaeal' membrane-bound nitrate reductases. *Fems Microbiology Letters* **276**, 129-139, doi:10.1111/j.1574-6968.2007.00887.x
10.1111/j.1574-6968.2007.00887.x. Epub 2007 Sep 20. (2007).
63 Kroninger, L., Berger, S., Welte, C. & Deppenmeier, U. Evidence for the involvement of two heterodisulfide reductases in the energy-conserving system of Methanomassiliicoccus luminyensis. *FEBS J* **283**, 472-483, doi:10.1111/febs.13594 (2016).
64 Einsle, O. *et al.* Structure of cytochrome c nitrite reductase. *Nature* **400**, 476-480, doi:10.1038/22802
10.1038/22802. (1999).
65 Hiratsuka, T. *et al.* An alternative menaquinone biosynthetic pathway operating in microorganisms. *Science* **321**, 1670-1673, doi:10.1126/science.1160446
10.1126/science.1160446. (2008).
66 Parks, D. H., Imelfort, M., Skennerton, C. T., Hugenholtz, P. & Tyson, G. W. CheckM: assessing the quality of microbial genomes recovered from isolates, single cells, and metagenomes. *Genome Research* **25**, 1043-1055, doi:10.1101/gr.186072.114
10.1101/gr.186072.114. Epub 2015 May 14. (2015).
67 Bowers, R. M. *et al.* Minimum information about a single amplified genome (MISAG) and a metagenome-assembled genome (MIMAG) of bacteria and archaea. *Nat Biotechnol* **35**, 725-731, doi:10.1038/nbt.3893 (2017).
68 Neumann, A., Wohlfarth, G. & Diekert, G. Tetrachloroethene dehalogenase from Dehalospirillum multivorans: cloning, sequencing of the encoding genes, and expression of the pceA gene in Escherichia coli. *J Bacteriol* **180**, 4140-4145 (1998).
69 Wrighton, K. C. *et al.* RubisCO of a nucleoside pathway known from Archaea is found in diverse uncultivated phyla in bacteria. *The ISME Journal* **10**, 2702-2714, doi:10.1038/ismej.2016.53
10.1038/ismej.2016.53. Epub 2016 May 3. (2016).

C Supplementary Tables and Figures

Suppl. Table 1: Overview of presence/absence of discussed enzymes in Asgard lineages

Suppl. Table 2: Annotations for proteins, which serve as candidate enzymes potentially involved in the various metabolic pathways discussed throughout this manuscript.

Suppl. Table 3: Automatic annotation of all genes

Suppl. Table 4: Carbohydrate active enzymes, peptidases, esterases and information on extracellular localization

Suppl. Table 5: Annotation of beta-oxidation genes encoded by Asgard genomes per protein family/phylogeny.

Please note that all Suppl. Tables are provided in two separate excel files referred to as "S-Tables_1-4.xlsx" (includes Suppl. Tables 1-4) and "S-Table5.xlsx" (includes Suppl. Table 5; with each sheet corresponding to one particular protein family of enzymes involved in β-oxidation)

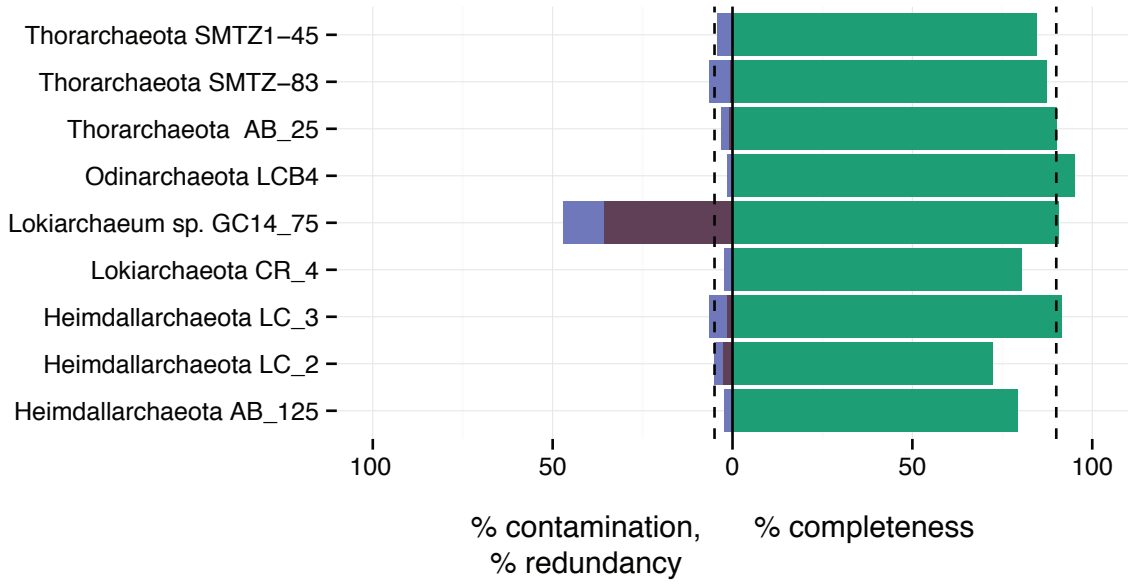

Suppl. Figure 1: Illustration of the quality of metagenome-assembled genomes (MAGs) of Asgard archaea

Barplot visualising the estimated completeness and contamination/redundancy values obtained with checkM[66] for the nine Asgard MAGs analysed in this work. The dashed line indicates the thresholds for contamination and completeness cutoffs representing high-quality MAGs according to the recently established metagenomic standards[67]. Two of the MAGs are of high quality according this criteria (Odinarchaeote LCB4 and Thorarchaeote AB_25), while the other MAGs represent medium quality bins. Purple bars represent the fraction of the contamination values (light blue bars) that is due to strain heterogeneity (redundant markers that share at least 90% of amino acid identity). As previously described in Spang et al. 2015[39], the Lokiarchaeum sp. GC14_75 MAG contains sequences from closely related strains, which explains the high contaminations/redundancy values observed in this MAG.

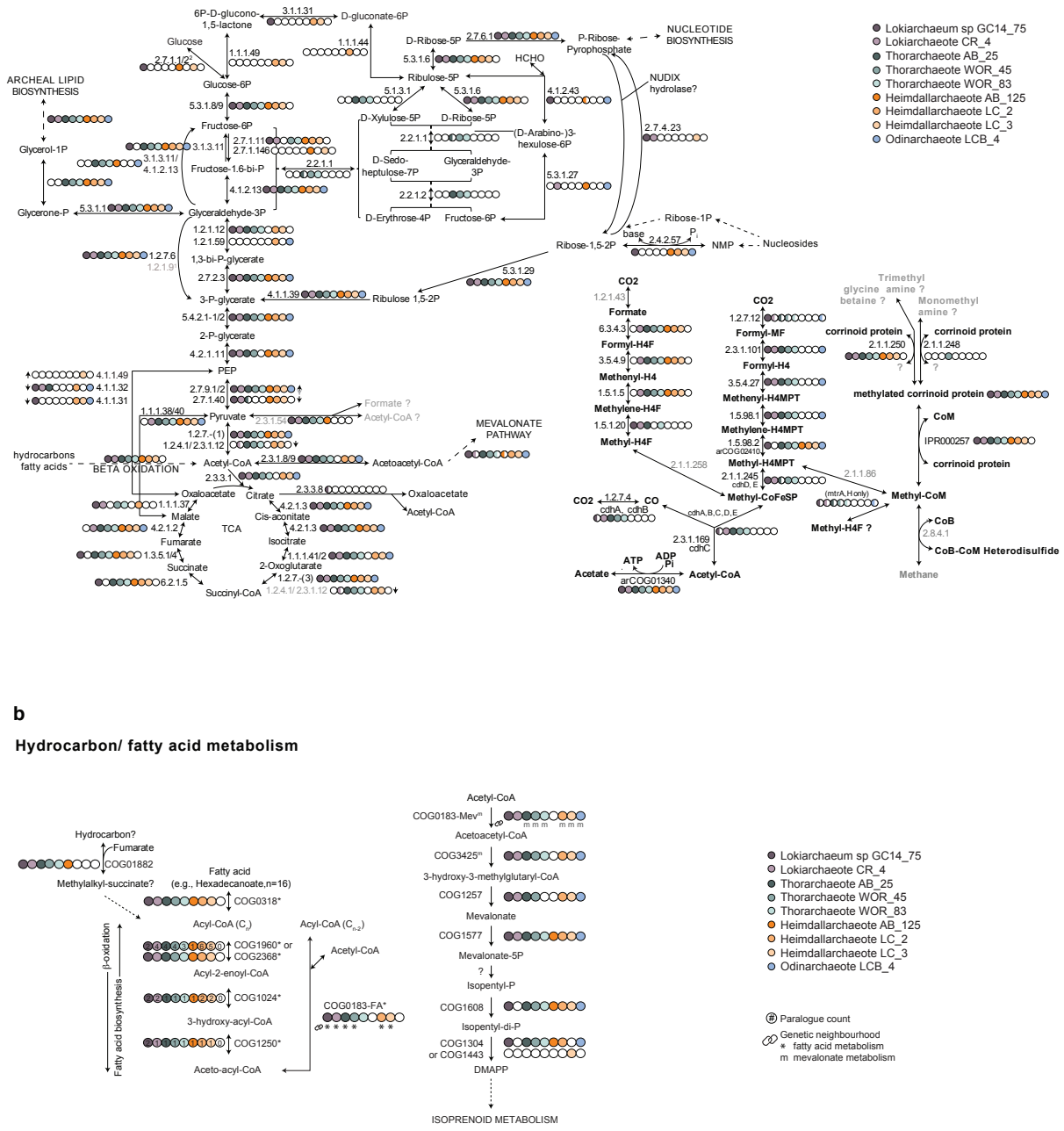

Suppl. Figure 2: Metabolic map of central carbon and lipid metabolism of Asgard archaea

For each enzyme, the corresponding enzyme commission (E.C.) or COG are provided and can be cross referenced in Suppl. Table 1 and 2. Coloured circles indicate the genomes in which homologues were detected, Lokiarchaeota (shades of purple), Thorarchaeota (shades of green), Heimdallarchaeota (shades of orange) and Odinarchaeota

(blue). a, Central carbon metabolism in Asgard archaea. b, left panel, Proposed CoA-coupled β-oxidation and fatty acid biosynthesis pathways of the Asgard archaea. For β-oxidation (counter-clockwise), fatty acids (e.g., Hexadecanoate) are activated with a long chain fatty acid CoA ligase (COG0318) generating an acyl-CoA species which is oxidized by a chain-length specific acyl-CoA dehydrogenase (COG1960) or 4-hydroxybutyryl-CoA dehydratase (COG2368). The resulting acyl-2-enoyl-CoA is further oxidized by enoyl-CoA hydratase (COG1024) and 3-hydroxy-acyl-CoA dehydrogenase (COG1250) to generate aceto-acyl-CoA which is ultimately cleaved by a B-ketothiolase/acetyl-CoA acetyltransferase (COG0183-FA) to generate acetyl-CoA and a Cn-2 acyl-CoA chain. Asterisks indicate that at least one B-ketothiolase/acetyl-CoA orthologue in the represented genome was encoded within 15 genes of one or more genes related to fatty acid metabolism (COG0318, COG1960, COG2368, COG1024, or COG1250). For complex protein families, the number of paralogues identified are shown in each circle. Fatty acid biosynthesis is depicted as the reverse of β-oxidation (clockwise) using CoA[33] and not acyl-carrier protein as an acyl carrier. b, right panel, Proposed mevalonate biosynthesis pathway. Acetyl-CoA is consecutively acetylated by the actions of B-ketothiolase/acetyl-CoA acetyltransferase (COG0183-Mev) and 3-hydroxy-3-methylglutaryl-CoA (HMG-CoA) synthase (COG3425) to produce HMG-CoA which in turn is converted to mevalonate by HMG-CoA reductase (COG1257). Mevalonate is phosphorylated by mevalonate kinase (COG1577) and converted to isopentyl-phosphate by an unknown enzyme. Isopentyl-phosphate is phosphorylated by isopentyl-phosphate kinase (COG1608) to isopentyl-di-phosphate which is isomerized to dimethylallyl pyrophosphate (DMAPP) by isopentyl-diphosphate isomerase 1 (COG1443) or 2 (COG1304). 'm' indicates that the COG0183 orthologue was encoded within 15 genes of the HMG-CoA synthase (COG3425). Greyed out text indicates: presence unclear, putative.

Group 4 [NiFe]-hydrogenase

Ca. Odinarchaeota archaeon LCB_4 – Group 4 [NiFe]-hydrogenase (OdinLCB4_14520)

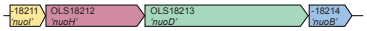

Ca. Odinarchaeota archaeon LCB_4 – Group 4 [NiFe]-hydrogenase (OdinLCB4_14620)

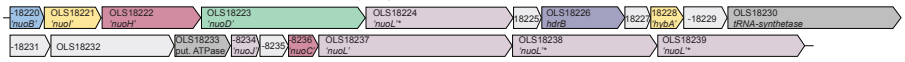

Ca. Odinarchaeota archaeon LCB_4 – Group 4 [NiFe]-hydrogenase (OdinLCB4_02560)

Ca. Heimdallarchaeota archaeon AB_125 – Group 4 [NiFe]-hydrogenase (HeimAB125_01550)

Ca. Heimdallarchaeota archaeon LC_2 – Group 4 [NiFe]-hydrogenase (HeimC2_23020)

Group 3c [NiFe]-hydrogenase

Ca. Lokiarchaeota archaeon GC14_75 – partial Group 3c [NiFe]-hydrogenase (Lokiarch_45490)

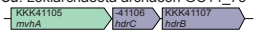

Ca. Lokiarchaeota archaeon GC14_75 – Group 3c [NiFe]-hydrogenase (Lokiarch_49310)

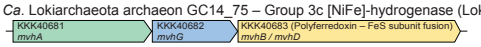

Ca. Lokiarchaeota archaeon CR_4 – Group 3c [NiFe]-hydrogenase (RBG13Loki_1669)

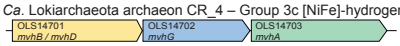

Ca. Thorarchaeota archaeon AB_25 – Group 3c [NiFe]-hydrogenase (ThorAB25_16580)

Ca. Thorarchaeota archaeon AB_25 – Group 3c [NiFe]-hydrogenase (ThorAB25_26490)

Ca. Thorarchaeota archaeon WOR_45 – Group 3c [NiFe]-hydrogenase (AM325_14150)

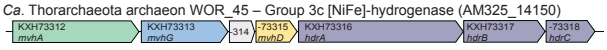

Ca. Thorarchaeota archaeon WOR_83 – Group 3c [NiFe]-hydrogenase (AM324_08070)

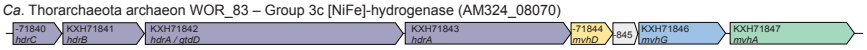

Ca. Heimdallarchaeota archaeon LC_2 – Group 3c [NiFe]-hydrogenase (HeimC2_23150)

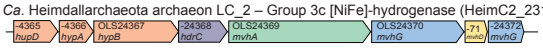

Ca. Heimdallarchaeota archaeon LC_3 – Group 3c [NiFe]-hydrogenase (HeimC3_04360)

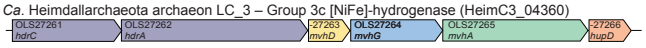

Group 3b [NiFe]-hydrogenase

Ca. Lokiarchaeota archaeon GC14_75 – partial Group 3b [NiFe]-hydrogenase (Lokiarch_31190)

Ca. Odinarchaeota archaeon LCB_4 – Group 3b [NiFe]-hydrogenase (OdinLCB4_08000)

Ca. Thorarchaeota archaeon WOR_45 – Group 3b [NiFe]-hydrogenase (AM325_05810)

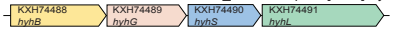

Ca. Thorarchaeota archaeon WOR_83 – Group 3b [NiFe]-hydrogenase (AM324_16110)

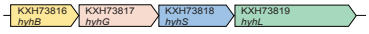

Ca. Heimdallarchaeota archaeon LC_3 – Group 3b [NiFe]-hydrogenase (HeimC3_04260)

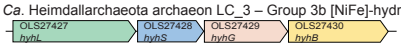

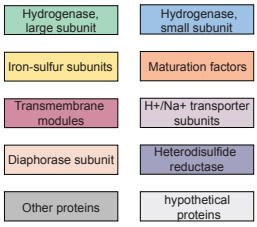

Suppl. Figure 3: Structure of [NiFe]-hydrogenase gene clusters. Genes were classified based on their top hits to the Conserved Domain Database (CDD) webserver and comparison of their sequences with those of hydrogenase operons represented in the hydrogenase database (HydDB). All genes are drawn to scale. Short gene names are given in italic and are shown in quotes whenever they are distantly related to known proteins. For group 4 [NiFe]-hydrogenases, the homologous genes to Nuo (Complex I; NADH-quinone oxidoreductase) are shown, with the more divergent *nuoL* homologs asterisked. Abbreviations are as follows: hdr, heterodisulfide reductase; hyh, hyperthermophile hydrogenase (group 3b [NiFe]-hydrogenase); mvh, methyl-viologen-reducing hydrogenase (group 3c [NiFe]-hydrogenase); hyp, Hydrogenase maturation factor; nuo, NADH dehydrogenase. [1]Note that this gene cluster is located at the end of the contig and thus incomplete. *NuoL*-like subunits are encoded on other short contigs, which are part of the *Heimdallarchaeum* AB125 genome. Thus, the encoded Group 4 [NiFe]-hydrogenase of this organism is most likely also ion conductive. Please note that also other gene clusters could be incomplete due to their location at the end of a contig.

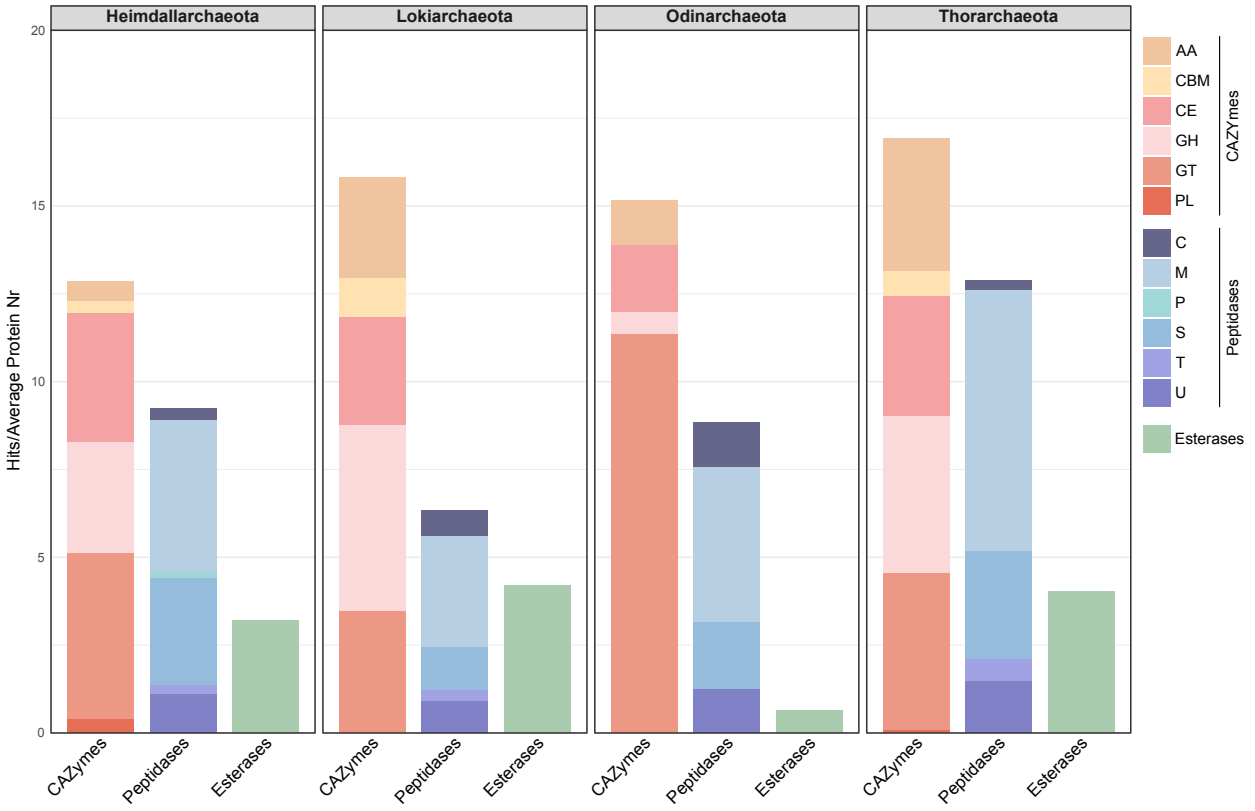

Suppl. Figure 4: Abundance of carbohydrate-active enzymes, peptidases and esterases in the Asgard genomes

Carbohydrate-active enzymes (CAZYmes), peptidases and esterases were identified in Asgard genomes using the dbCAN webserver, MEROPs and ESTER databases respectively (see Method section for details). Count data was averaged across the number of genomes represented by each phylum and normalized by the average number of proteins detected in each phylum. AA, auxiliary activities; CBM, carbohydrate-binding module; CE, carbohydrate esterase; GH, glycoside hydrolase; GT, glycosyltransferases; PL, polysaccharide lyase. A, aspartic peptidase; C, cysteine peptidase; M, metallopeptidase; P, mixed peptidase; S, serine peptidases; T, mixed catalytic type; U, Unknown Catalytic Type. Count data is summarized in Suppl. Table 4.

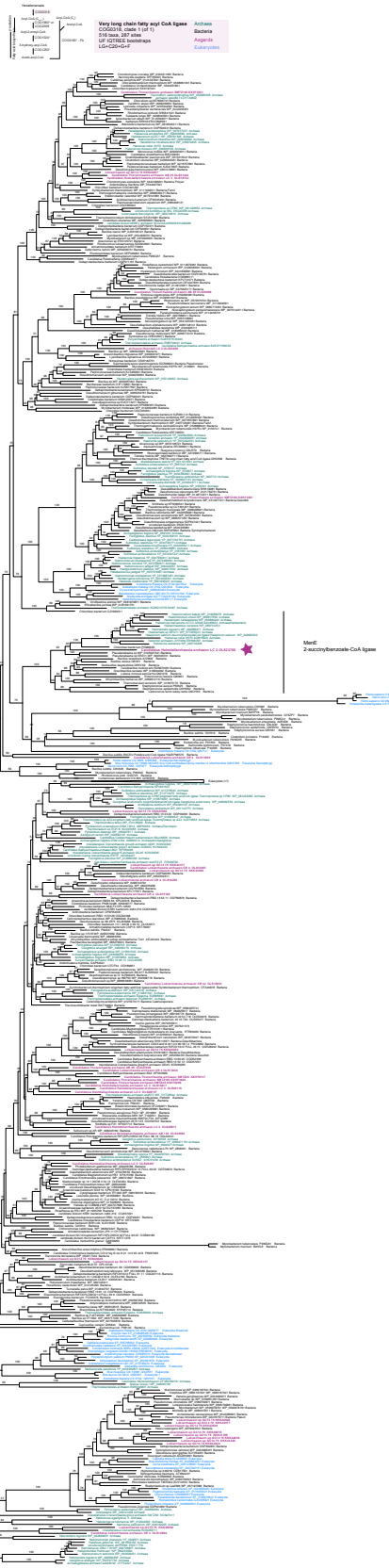
Very long chain fatty acyl CoA ligase
COG0318, clade 1 (of 1)
516 taxa, 267 sites
LG+C20+G+F
Archaea
Bacteria
Aegean.tb
Eukaryotes
MenE:
2-succinylbenzoate-CoA ligase

Suppl. Figure 5: Phylogenetic analysis of long chain fatty acid CoA ligase (COG0318). An unrooted phylogenetic tree was generated using IQ-tree LG+C20+F on an alignment of 516 taxa and 287 sites. Bacteria, Archaea, eukaryotes and Asgard archaea are colored in black, green, blue and purple respectively. Heimdallarchaeota MenE-like homologue is indicated with a star. Raw data files are available via figshare (see Data availability for more details).

Suppl. Figure 6: Asgard archaea have a versatile repertoire of Acyl-CoA dehydrogenases (COG1960). The acyl-CoA dehydrogenase family was subdivided into three large clades (a-c) based on preliminary phylogenetic analysis of sequences retrieved from Swigonova et al. 2009 and the best BLAST hits for each ASGARD sequences. Each unrooted tree was estimated using IQ-tree LG+C20+F for a) Clade 1 (117 taxa, 365 sites), b) Clade 2 (542 taxa, 311 sites), and c) Clade 3 (419 taxa, 300 sites) independently. Bacteria, Archaea, eukaryotes and Asgard archaea are colored in black, green, blue and purple, respectively. Bipartition support values are depicted as open or closed circles for ultra-fast bootstrap values greater than 70 and 90, respectively. A summary of the clade distribution among Asgard

genomes is shown in d. d) Clade summaries for each Asgard genome. Raw data files are available via figshare (see Data availability for more details).

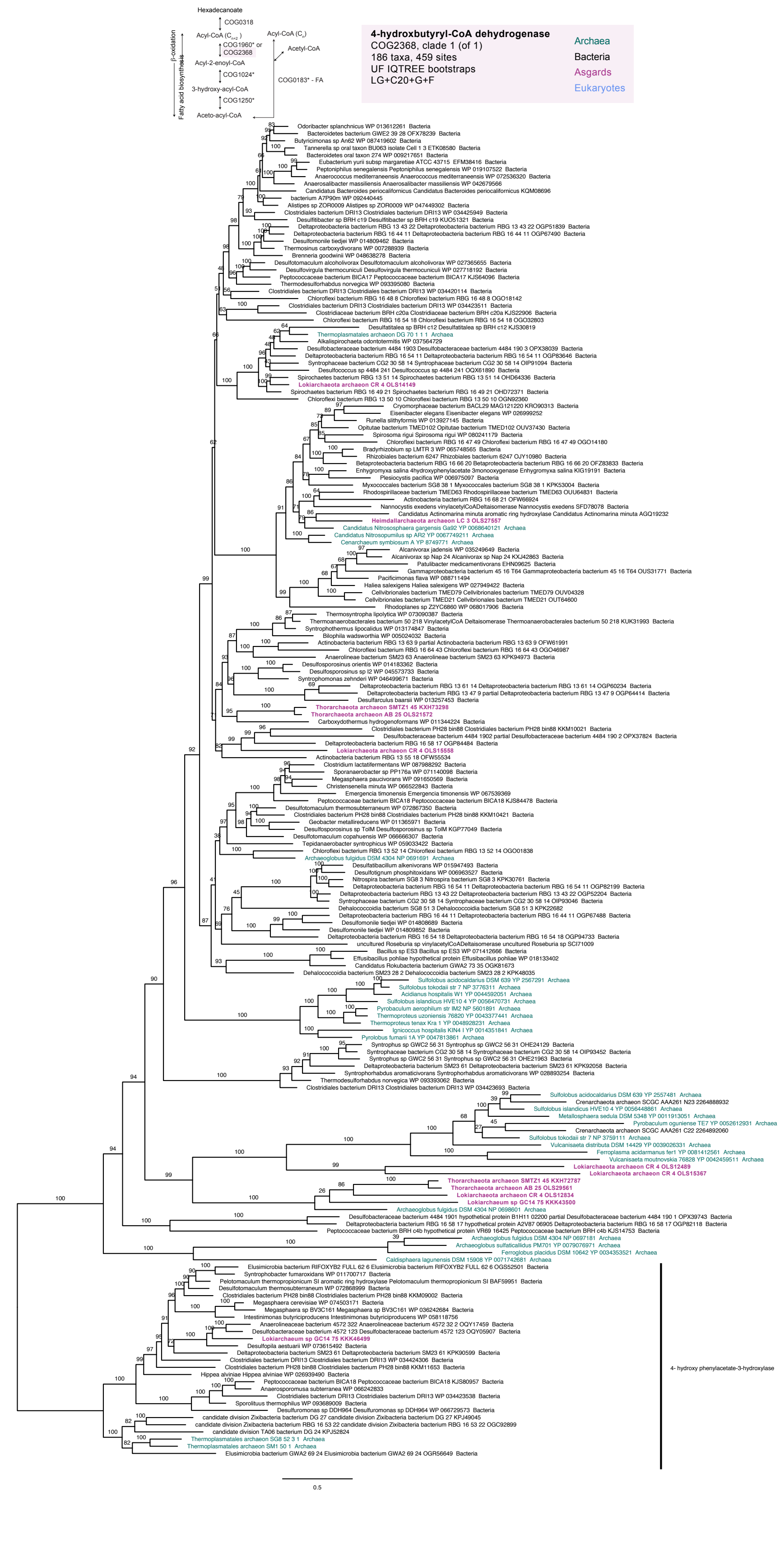
4-hydroxbutyryl-CoA dehydrogenase
COG2368, clade 1 (of 1)
186 taxa, 459 sites
UF IQTREE bootstraps
LG+C20+G+F
Archaea
Bacteria
Asgards
Eukaryotes
Hexadecanoate
COG0318
COG1960* or COG2368
COG1024*
COG1250*
COG0183* - FA
Acetyl-CoA
Acyl-2-enoyl-CoA
3-hydroxy-acyl-CoA
Aceto-acyl-CoA
β-oxidation
Fatty acid biosynthesis
4- hydroxy phenylacetate-3-hydroxylase
0.5

Suppl. Figure 7: Phylogenetic analysis of 4-hydroxy-butyryl-CoA dehydrogenases (COG2368). Phylogenetic tree was estimated using IQ-tree LG+C20+F on an alignment of 186 taxa and 459 sites and is unrooted. Bacteria, Archaea, eukaryotes and Asgards are colored in black, green, blue and purple, respectively. Raw data files are available via figshare (see Data availability for more details).

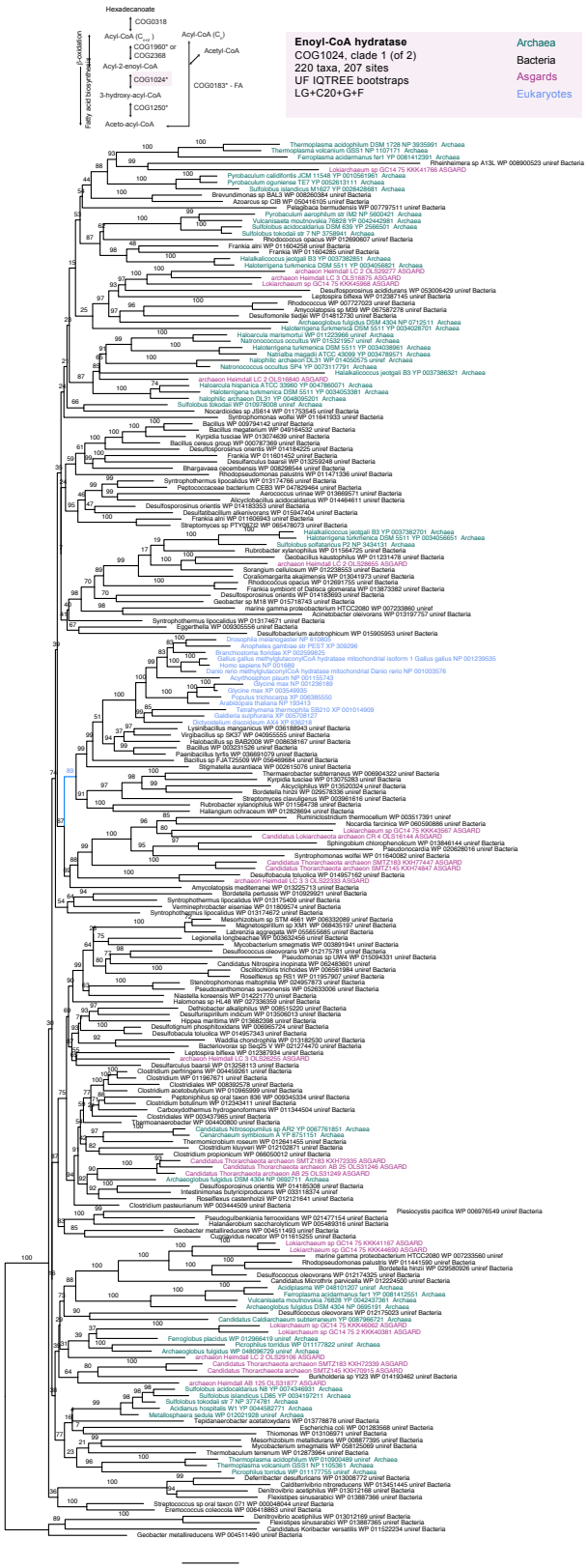
Hexadecanoate
COG0318
Acyl-CoA (C_{n+2})
COG1960* or COG2368
Acyl-2-enoyl-CoA
COG1024*
3-hydroxy-acyl-CoA
COG1250*
Aceto-acyl-CoA
Acyl-CoA (C_n)
Acetyl-CoA
COG0183* - FA
β-oxidation
Fatty acid biosynthesis
Enoyl-CoA hydratase
COG1024, clade 1 (of 2)
220 taxa, 207 sites
UF IQTREE bootstraps
LG+C20+G+F
Archaea
Bacteria
Asgards
Eukaryotes
0.5

Suppl. Figure 8: Phylogenetic analysis of Enoyl-CoA reductase clade 1 (COG1024). Phylogenetic tree was estimated using IQ-tree LG+C20+F on an alignment of 220 taxa and 207 sites and is unrooted. Bacteria, Archaea, eukaryotes and Asgards are colored in black, green, blue and purple respectively. Raw data files are available via figshare (see Data availability for more details).

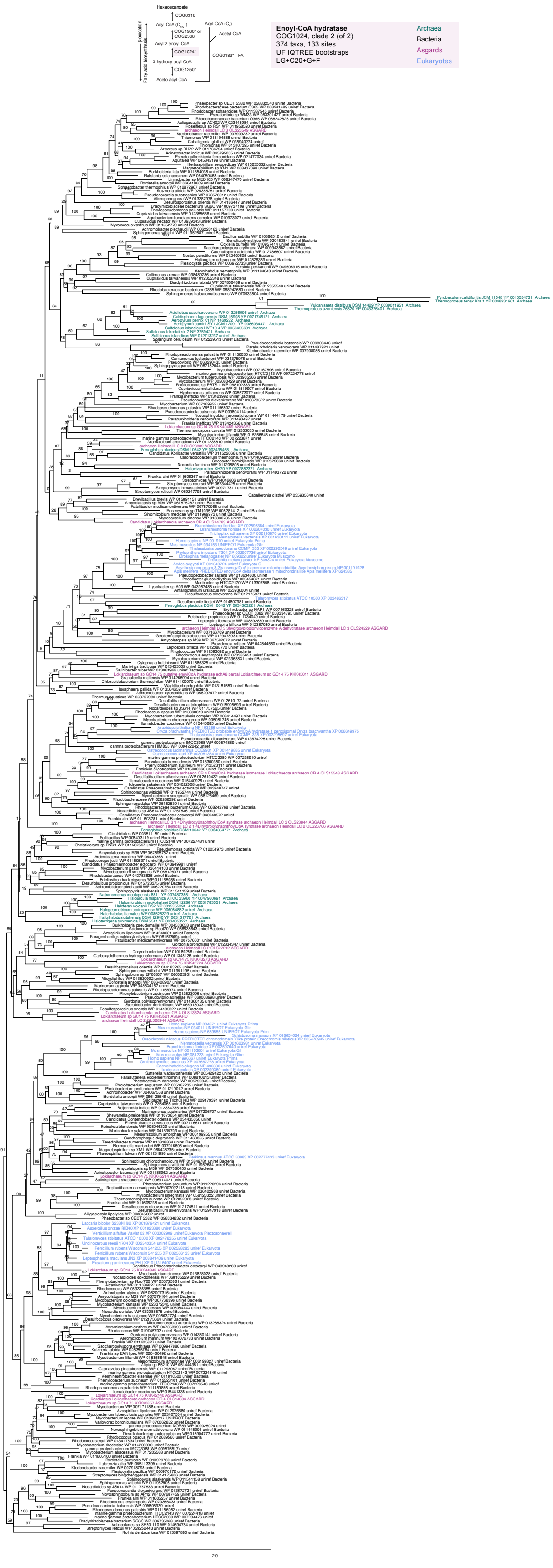
Hexadecanoate
COG0318
Acyl-CoA (C_{n+2})
COG1960* or COG2368
Acyl-2-enoyl-CoA
COG1024*
3-hydroxy-acyl-CoA
COG1250*
Aceto-acyl-CoA
Acyl-CoA (C_n)
Acetyl-CoA
COG0183* - FA
β-oxidation
Fatty acid biosynthesis
Enoyl-CoA hydratase
COG1024, clade 2 (of 2)
374 taxa, 133 sites
UF IQTREE bootstraps
LG+C20+G+F
Archaea
Bacteria
Asgards
Eukaryotes
2.0

Suppl. Figure 9: Phylogenetic analysis of Enoyl-CoA reductase clade 2 (COG1024). Phylogenetic tree was estimated using IQ-tree LG+C20+F on an alignment of 374 taxa and 133 sites and is unrooted. Bacteria, Archaea, eukaryotes and Asgards are colored in black, green, blue and purple respectively. Raw data files are available via figshare (see Data availability for more details).


Hexadecanoate
Acyl-CoA (C_)
Acyl-CoA (C_)
Acetyl-CoA
Acyl-enoyl-CoA
3-hydroxy-acyl-CoA
Acetoacetyl-CoA
FA elongation cycle (4 steps)
3-hydroxyacyl-CoA dehydrogenase
Archaea
Bacteria
Eukaryotes
Asgards
0.4

Suppl. Figure 10: Phylogenetic analysis of 3-hydroxy-acyl-CoA dehydrogease (COG1250). Phylogenetic tree was estimated using IQ-tree LG+C20+F on an alignment of 288 taxa and 240 sites and is unrooted. Bacteria, Archaea, eukaryotes and Asgards are colored in black, green, blue and purple respectively. Raw data files are available via figshare (see Data availability for more details).

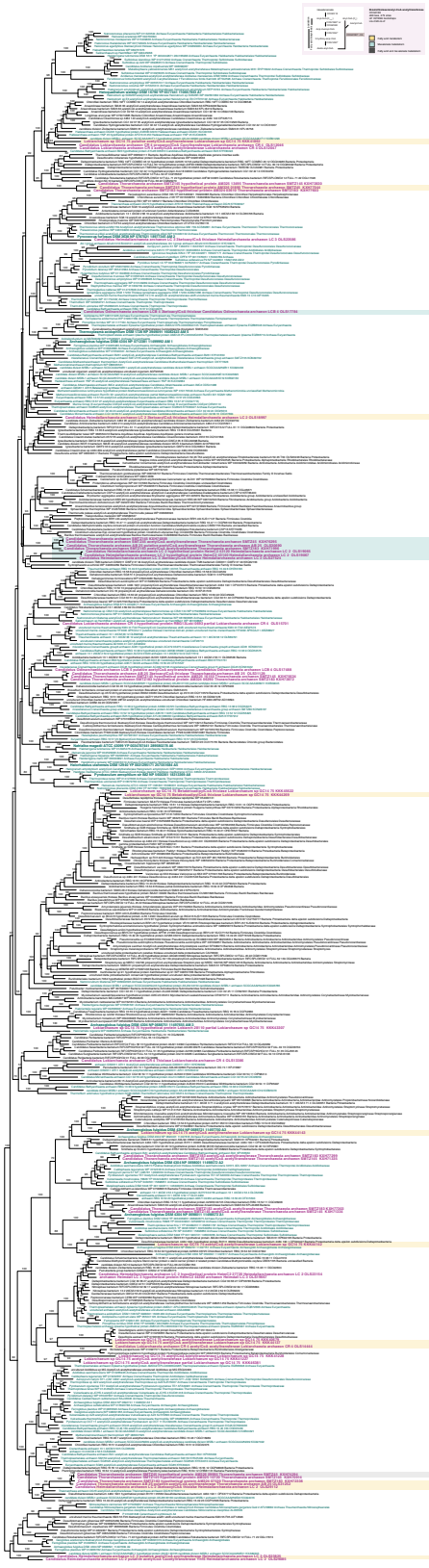
Clade 1A
Clade 1B
Clade 1C
Clade 1D
Clade 1E
Clade 1F
Clade 1G
Clade 1H
Clade 1I
Clade 1J
Clade 1K
Clade 1L
Clade 1M

Suppl. Figure 11: Phylogenetic analysis of clade 1 of B-ketothiolase/acetyl-CoA acetyltransferase (COG0183). Phylogenetic tree was estimated using IQ-tree LG+C20+F on an alignment of 466 taxa and 279 sites. Bacteria, Archaea, and Asgards are colored in black, green, and purple respectively. Gene sequences from Asgard that are genetically linked to fatty acid metabolism or mevalonate metabolism or both fatty acid and mevalonate metabolism are shown in yellow, green and grey respectively summarized in Suppl. Figure 13. Raw data files are available via figshare (see Data availability for more details).

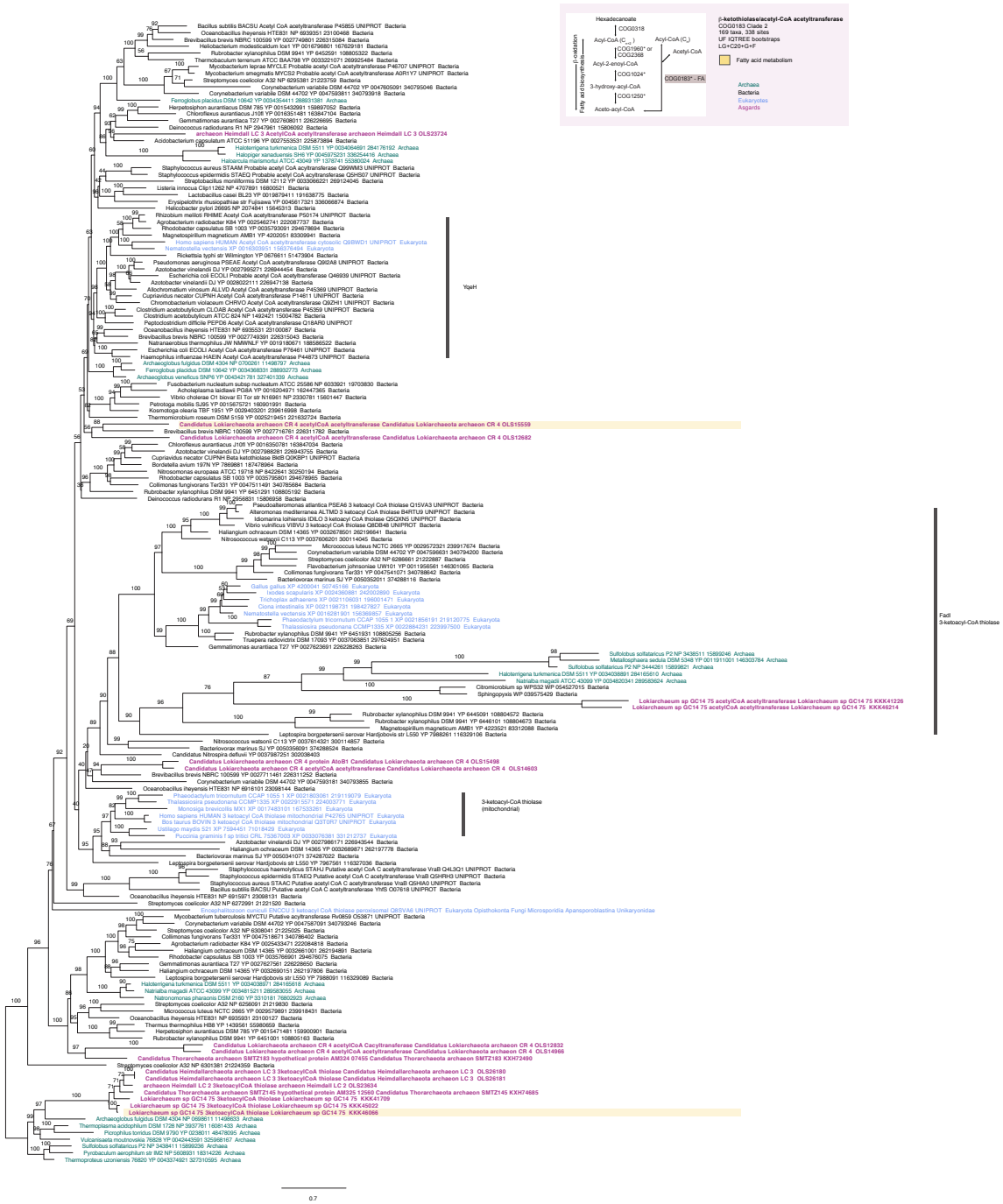
Hexadecanoate
COG0318
Acyl-CoA (C16)
COG1960* or COG2368
Acyl-CoA (C4)
Acetyl-CoA
Acyl-2-enoyl-CoA
COG1024*
COG0183* - FA
3-hydroxy-acyl-CoA
COG1250*
Aceto-acyl-CoA
β-oxidation
Fatty acid biosynthesis
β-ketothiolase/acetyl-CoA acetyltransferase
COG0183 Clade 2
169 taxa, 338 sites
UF IQTREE bootstraps
LG+C20+G+F
Fatty acid metabolism
Archaea
Bacteria
Eukaryotes
Asgards
YqeH
FadI
3-ketoacyl-CoA thiolase
3-ketoacyl-CoA thiolase (mitochondrial)
0.7

Suppl. Figure 12: Phylogenetic analysis of clade 2 of B-ketothiolase/acetyl-CoA acetyltransferase (COG0183). Phylogenetic tree was estimated using IQ-tree LG+C20+F on an alignment of 169 taxa and 338 sites. Bacteria, Archaea, and Asgards are coloured in black, green, and purple respectively. Gene sequences from Asgard that are genetically linked to fatty acid metabolism yellow and summarized in Suppl. Figure 13. Raw data files are available via figshare (see Data availability for more details).

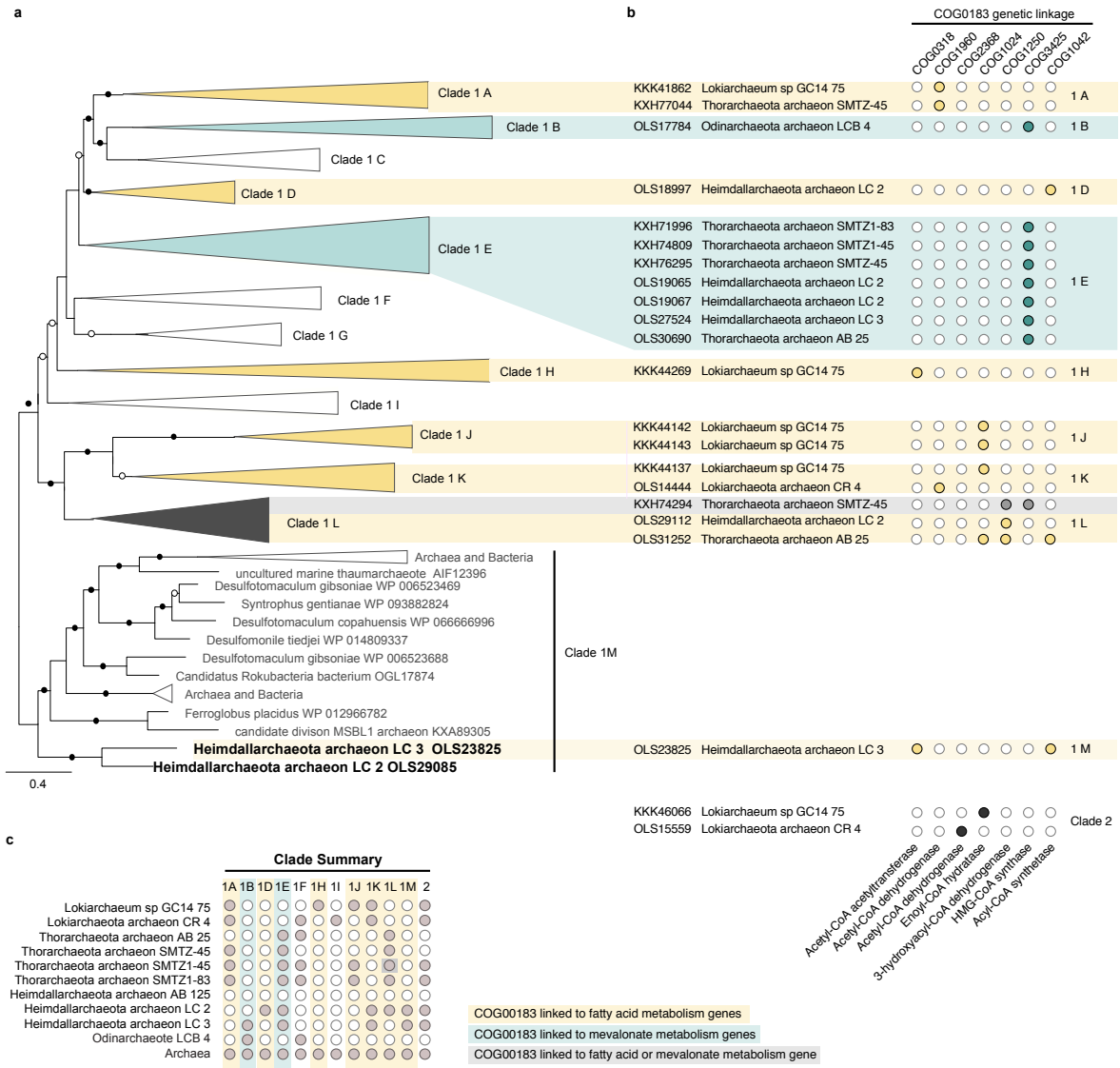

Suppl. Figure 13: Phylogenetic and gene linkage analysis of B-ketothiolase/acetyl-CoA acetyltransferase (COG0183). a, The COG0183 protein family was divided into two clades based on previous reports by[33] where clade 1 is composed of mostly archaeal sequences previously implicated in fatty acid and mevalonate metabolism. A schematic representation of clade 1 based on a tree constructed with IQ-tree LG+C20+F on an alignment of 466 taxa and 279 sites and unrooted. Bipartition support values are depicted as open or closed circles for ultra-fast bootstrap values greater than 70 and 90 respectively. Full phylogeny can be found in Suppl. Figs 10, 11. b, Gene sequences from Asgard archaea that are genetically linked (i.e., within 15 genes of the B-ketothiolase/acetyl-CoA acetyltransferase gene) to the indicated fatty acid metabolism or mevalonate metabolism or both fatty acid and mevalonate metabolism are shown in yellow, green and grey respectively. c, Distribution of Asgard archaeal sequences in each subclade. Raw data files are available via figshare (see Data availability for more details).

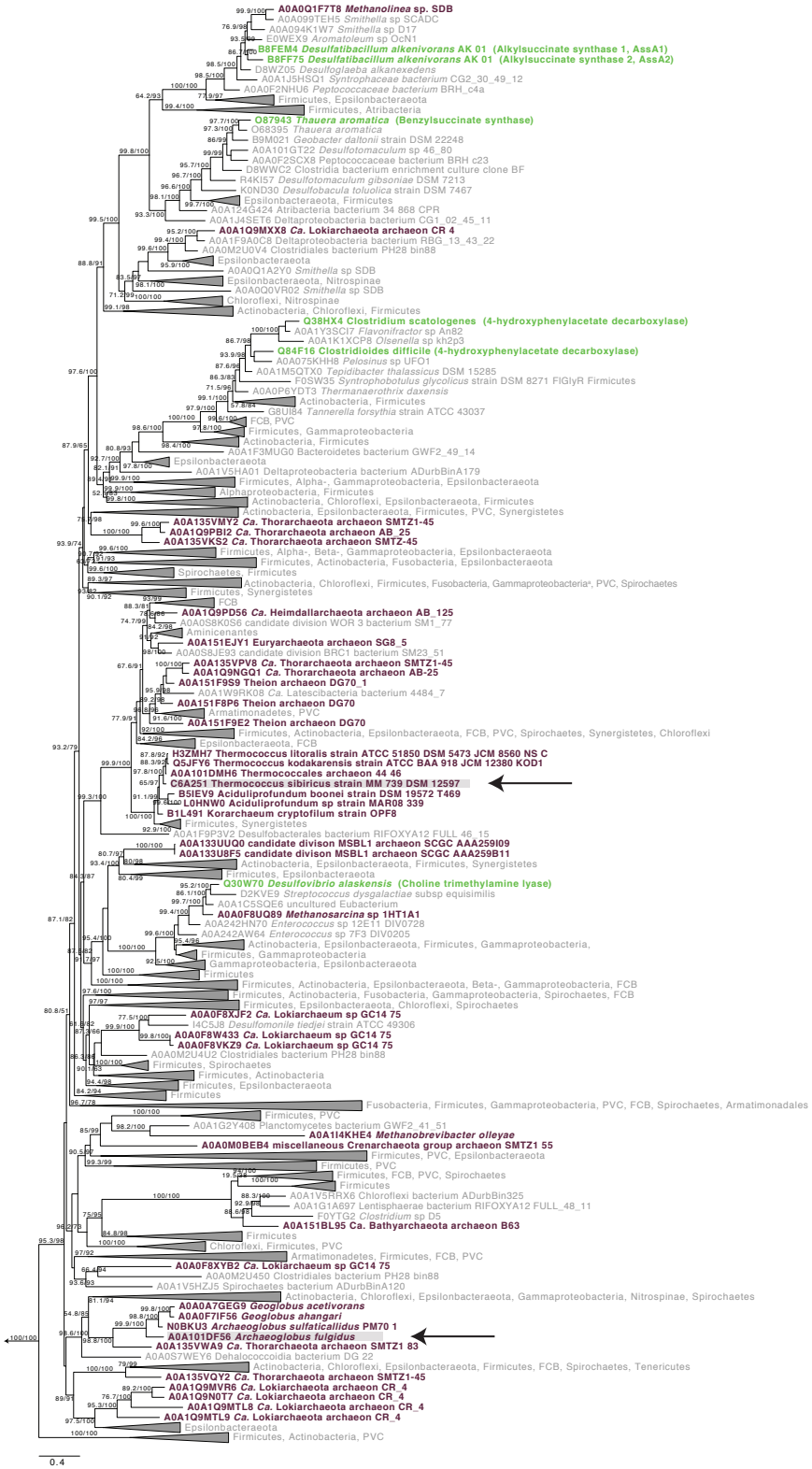
A0A0Q1F7T8 Methanolinea sp. SDB
A0A099TEH5 Smithella sp SCADC
A0A094K1W7 Smithella sp D17
E0WEX9 Aromatoleum sp OcN1
B8FEM4 Desulfatibacillum alkenivorans AK 01 (Alkylsuccinate synthase 1, AssA1)
B8FF75 Desulfatibacillum alkenivorans AK 01 (Alkylsuccinate synthase 2, AssA2)
D8WZ05 Desulfoglaeba alkanexedens
A0A1J5HSQ1 Syntrophaceae bacterium CG2_30_49_12
A0A0F2NHU6 Peptococcaceae bacterium BRH_c4a
Firmicutes, Epsilonbacteraeota
Firmicutes, Atribacteria
O87943 Thauera aromatica (Benzylsuccinate synthase)
O68395 Thauera aromatica
B9M021 Geobacter daltonii strain DSM 22248
A0A101GT22 Desulfotomaculum sp 46_80
A0A0F2SCX8 Peptococcaceae bacterium BRH c23
D8WWC2 Clostridia bacterium enrichment culture clone BF
R4KI57 Desulfotomaculum gibsoniae DSM 7213
K0ND30 Desulfobacula toluolica strain DSM 7467
Epsilonbacteraeota, Firmicutes
A0A124G424 Atribacteria bacterium 34 868 CPR
A0A1J4SET6 Deltaproteobacteria bacterium CG1_02_45_11
A0A1Q9MXX8 Ca. Lokiarchaeota archaeon CR 4
A0A1F9A0C8 Deltaproteobacteria bacterium RBG_13_43_22
A0A0M2U0V4 Clostridiales bacterium PH28 bin88
Epsilonbacteraeota
A0A0Q1A2Y0 Smithella sp SDB
Epsilonbacteraeota, Nitrospinae
A0A0Q0VR02 Smithella sp SDB
Chloroflexi, Nitrospinae
Actinobacteria, Chloroflexi, Firmicutes
Q38HX4 Clostridium scatologenes (4-hydroxyphenylacetate decarboxylase)
A0A1Y3SCI7 Flavonifractor sp An82
A0A1K1XCP8 Olsenella sp kh2p3
Q84F16 Clostridioides difficile (4-hydroxyphenylacetate decarboxylase)
A0A075KHH8 Pelosinus sp UFO1
A0A1M5QTX0 Tepidibacter thalassicus DSM 15285
F0SW35 Syntrophobotulus glycolicus strain DSM 8271 FlGlyR Firmicutes
A0A0P6YDT3 Thermanaerothrix daxensis
Actinobacteria, Firmicutes
G8UI84 Tannerella forsythia strain ATCC 43037
FCB, PVC
Firmicutes, Gammaproteobacteria
Actinobacteria, Firmicutes
A0A1F3MUG0 Bacteroidetes bacterium GWF2_49_14
Epsilonbacteraeota
A0A1V5HA01 Deltaproteobacteria bacterium ADurbBinA179
Firmicutes, Alpha-, Gammaproteobacteria, Epsilonbacteraeota
Alphaproteobacteria, Firmicutes
Actinobacteria, Chloroflexi, Epsilonbacteraeota, Firmicutes
Actinobacteria, Epsilonbacteraeota, Firmicutes, PVC, Synergistetes
A0A135VMY2 Ca. Thorarchaeota archaeon SMTZ1-45
A0A1Q9PBI2 Ca. Thorarchaeota archaeon AB_25
A0A135VKS2 Ca. Thorarchaeota archaeon SMTZ-45
Firmicutes, Alpha-, Beta-, Gammaproteobacteria, Epsilonbacteraeota
Firmicutes, Actinobacteria, Fusobacteria, Epsilonbacteraeota
Spirochaetes, Firmicutes
Actinobacteria, Chloroflexi, Firmicutes, Fusobacteria, Gammaproteobacteria[a], PVC, Spirochaetes
Firmicutes, Synergistetes
FCB
A0A1Q9PD56 Ca. Heimdallarchaeota archaeon AB_125
A0A0S8K0S6 candidate division WOR 3 bacterium SM1_77
Aminicenantes
A0A151EJY1 Euryarchaeota archaeon SG8_5
A0A0S8JE93 candidate division BRC1 bacterium SM23_51
A0A135VPV8 Ca. Thorarchaeota archaeon SMTZ1-45
A0A1Q9NGQ1 Ca. Thorarchaeota archaeon AB-25
A0A151F9S9 Theion archaeon DG70_1
A0A1W9RK08 Ca. Latescibacteria bacterium 4484_7
A0A151F8P6 Theion archaeon DG70
Armatimonadetes, PVC
A0A151F9E2 Theion archaeon DG70
Firmicutes, Actinobacteria, Epsilonbacteraeota, FCB, PVC, Spirochaetes, Synergistetes, Chloroflexi
Epsilonbacteraeota, FCB
H3ZMH7 Thermococcus litoralis strain ATCC 51850 DSM 5473 JCM 8560 NS C
Q5JFY6 Thermococcus kodakarensis strain ATCC BAA 918 JCM 12380 KOD1
A0A101DMH6 Thermococcales archaeon 44 46
C6A251 Thermococcus sibiricus strain MM 739 DSM 12597
B5IEV9 Aciduliprofundum boonei strain DSM 19572 T469
L0HNW0 Aciduliprofundum sp strain MAR08 339
B1L491 Korarchaeum cryptofilum strain OPF8
Firmicutes, Synergistetes
A0A1F9P3V2 Desulfobacterales bacterium RIFOXYA12 FULL 46_15
A0A133UUQ0 candidate division MSBL1 archaeon SCGC AAA259I09
A0A133U8F5 candidate division MSBL1 archaeon SCGC AAA259B11
Actinobacteria, Epsilonbacteraeota, Firmicutes, Synergistetes
Firmicutes, Epsilonbacteraeota
Q30W70 Desulfovibrio alaskensis (Choline trimethylamine lyase)
D2KVE9 Streptococcus dysgalactiae subsp equisimilis
A0A1C5SQE6 uncultured Eubacterium
A0A0F8UQ89 Methanosarcina sp 1HT1A1
A0A242HN70 Enterococcus sp 12E11 DIV0728
A0A242AW64 Enterococcus sp 7F3 DIV0205
Actinobacteria, Epsilonbacteraeota, Firmicutes, Gammaproteobacteria,
Firmicutes, Gammaproteobacteria
Gammaproteobacteria, Epsilonbacteraeota
Firmicutes
Firmicutes, Actinobacteria, Epsilonbacteraeota, Beta-, Gammaproteobacteria, FCB
Firmicutes, Actinobacteria, Fusobacteria, Gammaproteobacteria, Spirochaetes, FCB
Firmicutes, Epsilonbacteraeota, Chloroflexi, Spirochaetes
A0A0F8XJF2 Ca. Lokiarchaeum sp GC14 75
I4C5J8 Desulfomonile tiedjei strain ATCC 49306
A0A0F8W433 Ca. Lokiarchaeum sp GC14 75
A0A0F8VKZ9 Ca. Lokiarchaeum sp GC14 75
A0A0M2U4U2 Clostridiales bacterium PH28 bin88
Firmicutes, Spirochaetes
Firmicutes, Actinobacteria
Firmicutes, Epsilonbacteraeota
Firmicutes
Fusobacteria, Firmicutes, Gammaproteobacteria, PVC, FCB, Spirochaetes, Armatimonadales
Firmicutes, PVC
A0A1G2Y408 Planctomycetes bacterium GWF2_41_51
A0A1I4KHE4 Methanobrevibacter olleyae
A0A0M0BEB4 miscellaneous Crenarchaeota group archaeon SMTZ1 55
Firmicutes, PVC, Epsilonbacteraeota
Firmicutes, PVC
Firmicutes, FCB, PVC, Spirochaetes
Firmicutes
A0A1V5HRX6 Chloroflexi bacterium ADurbBin325
A0A1G1A697 Lentisphaerae bacterium RIFOXYA12 FULL_48_11
F0YTG2 Clostridium sp D5
A0A151BL95 Ca. Bathyarchaeota archaeon B63
Firmicutes
Chloroflexi, Firmicutes, PVC
Armatimonadetes, Firmicutes, FCB, PVC
A0A0F8XYB2 Ca. Lokiarchaeum sp GC14 75
A0A0M2U450 Clostridiales bacterium PH28 bin88
A0A1V5HZJ5 Spirochaetes bacterium ADurbBinA120
Actinobacteria, Chloroflexi, Epsilonbacteraeota, Gammaproteobacteria, Nitrospinae, Spirochaetes
A0A0A7GEG9 Geoglobus acetivorans
A0A0F7IF56 Geoglobus ahangari
N0BKU3 Archaeoglobus sulfaticallidus PM70 1
A0A101DF56 Archaeoglobus fulgidus
A0A135VWA9 Ca. Thorarchaeota archaeon SMTZ1 83
A0A0S7WEY6 Dehalococcoidia bacterium DG 22
Actinobacteria, Chloroflexi, Epsilonbacteraeota, Firmicutes, FCB, Spirochaetes, Tenericutes
A0A135VQY2 Ca. Thorarchaeota archaeon SMTZ1-45
A0A1Q9MVR6 Ca. Lokiarchaeota archaeon CR_4
A0A1Q9N0T7 Ca. Lokiarchaeota archaeon CR_4
A0A1Q9MTL8 Ca. Lokiarchaeota archaeon CR_4
A0A1Q9MTL9 Ca. Lokiarchaeota archaeon CR_4
Epsilonbacteraeota
Firmicutes, Actinobacteria, PVC
0.4

Suppl. Figure 14: Maximum likelihood phylogenetic analysis of pyruvate-formate lyase superfamily proteins. Phylogenetic tree was estimated using IQ-tree LG+C20+R+F and is based on a protein alignment of 336 aligned sites and includes 1012 sequences. Support values (SH-like approximate likelihood ratio test and ultrafast bootstraps) are not shown whenever one of the values was below 50. Scale bar indicates number of substitutions per site. Arrows point to proteins of organisms that are known to utilize hydrocarbons. Raw data files are available via figshare (see Data availability for more details).

Organohalides:
TCB, trichlorobenzene;
TeCB, tetrachlorobenzene;
PCE, perchloroethylene;
TCE, trichloroethylene;
DCE, dichloroethene;
DCP, dichlorophenol;
VC, vinyl chloride;
DCA, dichloroethane;
3Cl-4-HBA, 3-chloro-4-hydroxybenzoate.

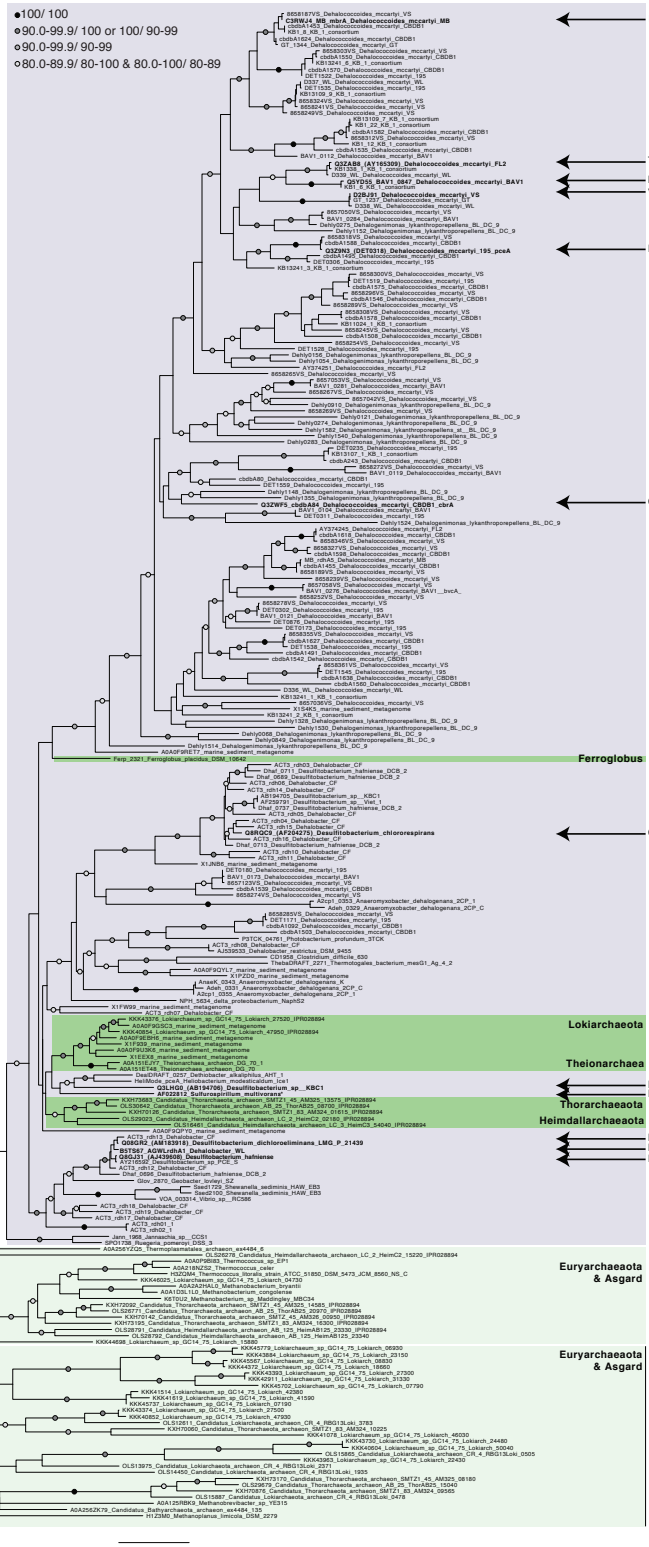

Suppl. Figure 15: Maximum likelihood phylogenetic analysis of reductive dehalogenases. Phylogenetic tree was estimated using IQ-tree LG+C40+R+F and is based on a protein alignment of 160 aligned sites and includes 243 sequences. All support values (SH-like approximate likelihood ratio test and ultrafast bootstraps) below 80 as well as support values of closely related sequences were removed to increase readability and are represented by filled circles according to the color code in the figure legend. Tree was rooted using midpoint rooting. Scale bar indicates the number of substitutions per site. Archaeal clades are shaded in green, bacteria are shaded in violet. Dark green shading refers to archaeal sequences that might represent *bona fide* reductive dehalogenases while the function of sequences highlighted in light green is less clear. The current outgroup represents homologous sequences of Asgard archaea assigned to COG1600 but lacking significant hit to reductive dehalogenase domains (IPR028894). However, notice that some archaeal sequences which encode IPR028894 cluster with these divergent Asgard sequences. The substrates of some know reductive dehalogenases are indicated based on[57,68] and the backbone dataset is based on sequences kindly provided by Laura Hug and described in[59]. Abr.: Organohalides: TCB, trichlorobenzene; TeCB, tetrachlorobenzene; PCE, perchloroethylene; TCE, trichloroethylene; DCE, dichloroethene; DCP, dichlorophenol; VC, vinyl chloride; DCA, dichloroethane; 3Cl-4-HBA, 3-chloro-4-hydroxybenzoate. *This sequence is 99% similar to W6EQP0, for which a X-ray crystal structure has been obtained[56]. Raw data files are available via figshare (see Data availability for more details).

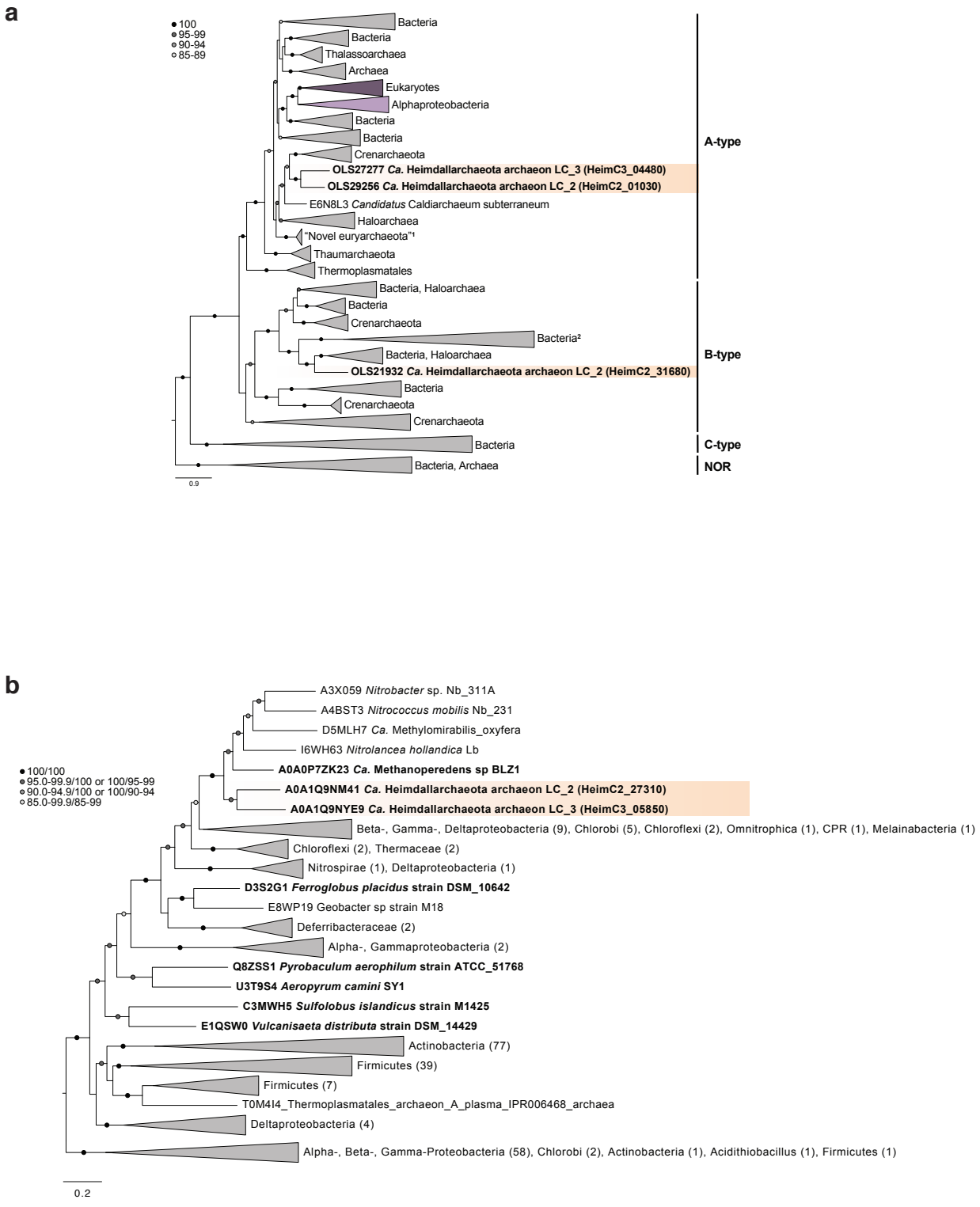

Suppl. Figure 16: Maximum likelihood phylogenetic analysis of Heme-copper-type cytochrome c oxidase, subunit 1 and nitrate reductase, alpha subunit. a, Phylogenetic tree of Heme-copper-type cytochrome c oxidase, subunit 1

was estimated using IQ-tree LG+C20 and is based on a protein alignment of 443 aligned sites and includes 1078 sequences. Only support values (ultrafast bootstraps) above 85 are shown and are represented by filled circles according to the color code in the figure legend. The tree was rooted using the distantly related nitric-oxide reductase (NOR). b, Phylogenetic tree of the alpha-subunit of the bacterial nitrate reductase family (IPR006468) was estimated using IQ-tree LLG+C20+F+R and is based on a protein alignment of 1071 aligned sites and including 233 sequences. Only support values (SH-like approximate likelihood ratio test and ultrafast bootstraps) above 80 are represented by filled circles according to the color code in the Fig. legend. The tree was rooted arbitrarily. a,b Scale bars indicate number of substitutions per site. Raw data files are available via figshare (see Data availability for more details).

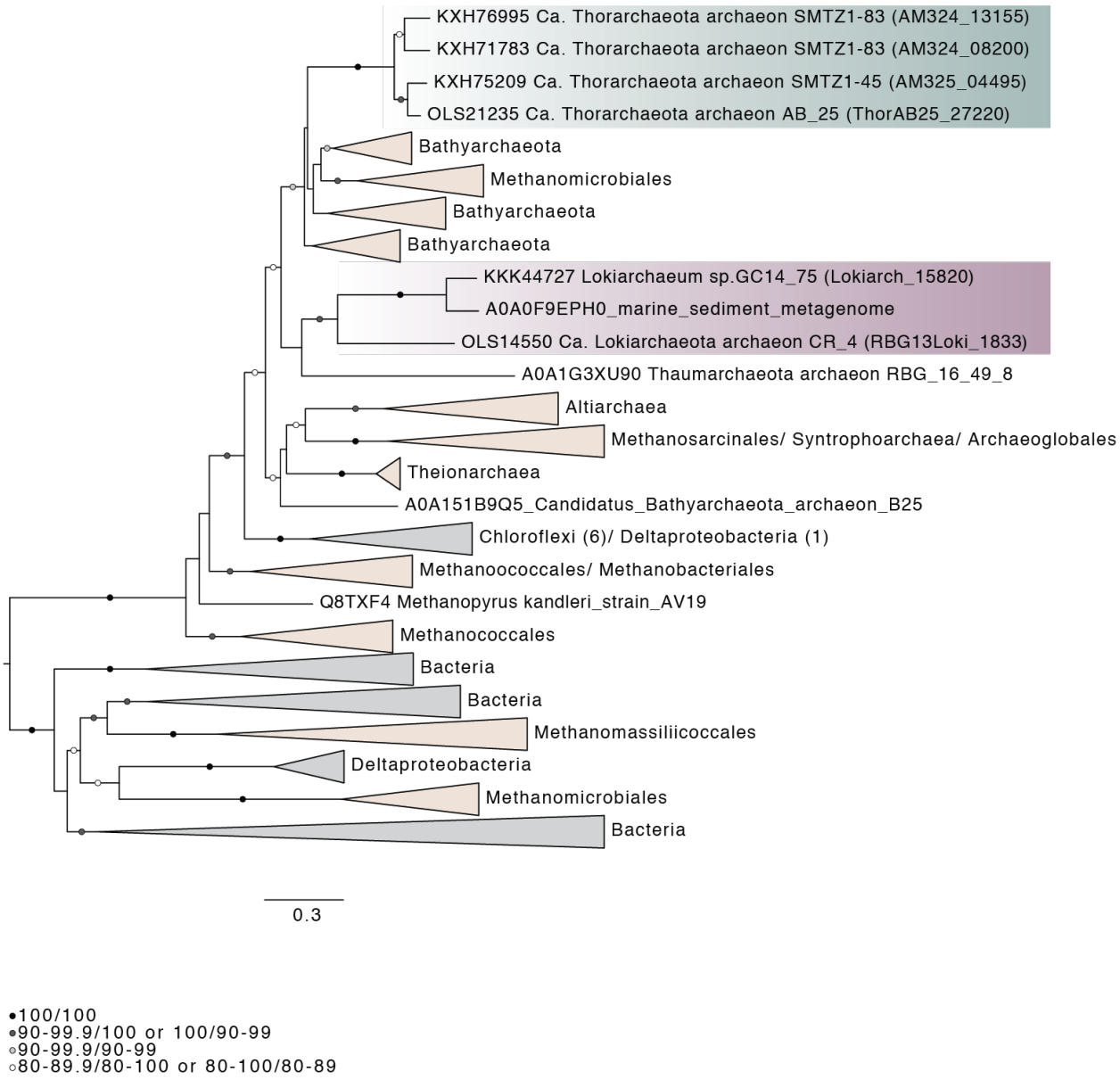

Suppl. Figure 17: Maximum likelihood phylogenetic analysis of key subunit of acetyl-CoA synthase/CO dehydrogenase. Phylogenetic tree was estimated for protein sequences with PF03598 encoding the key subunit of Acetyl-CoA synthase/CO dehydrogenase, cdhC (also referred to as CODH/acetyl-CoA synthase beta subunit or alpha subunit of ACS/CODH) using IQ-tree with the LG+C20+F+R. The protein alignment consisted of 712 aligned sites and includes 442 sequences. Only support values (SH-like approximate likelihood ratio test and ultrafast bootstraps) above 80 are represented by filled circles according to the color code in the figure legend. Scale bar indicates number of substitutions per site. Raw data files are available via figshare (see Data availability for more details).

a

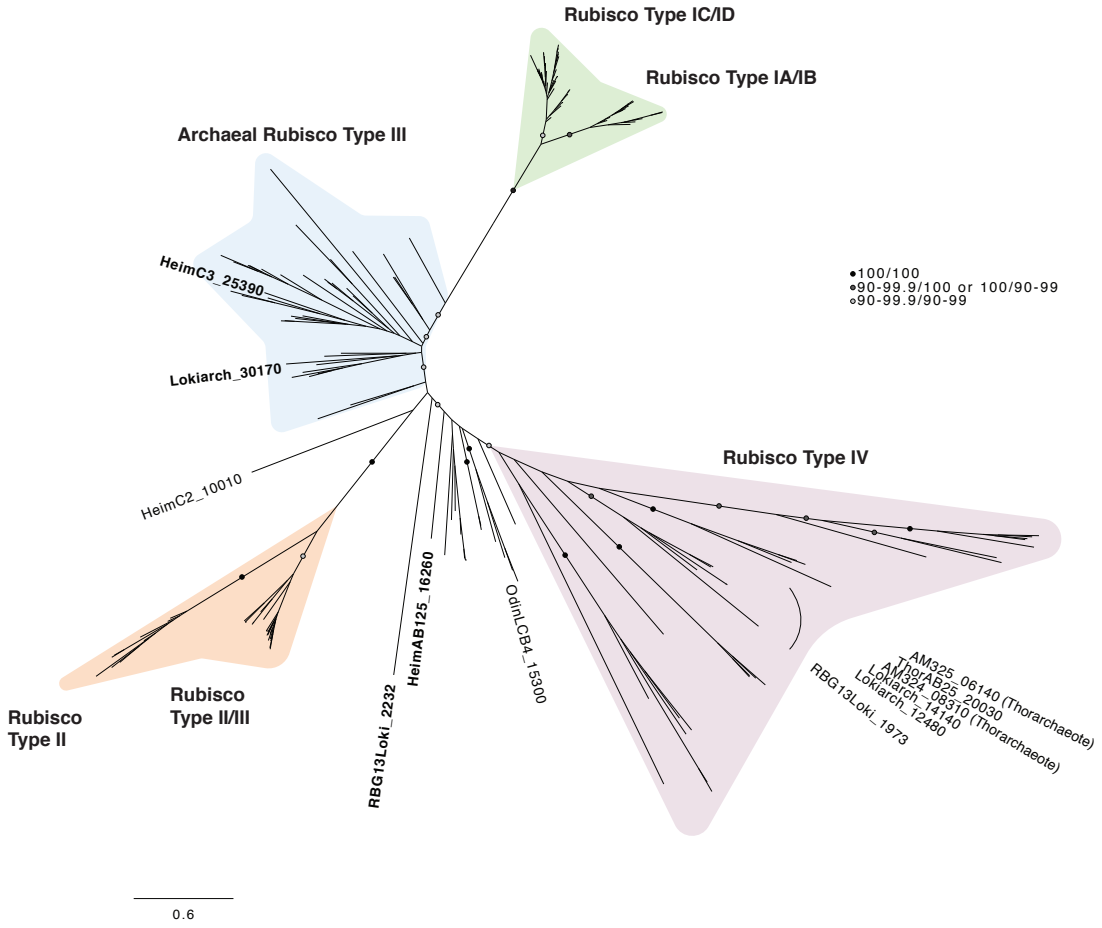

b

		57	52	120	172	174	176	195	196	198	200	201	291	292	324	331	376	377	400	401
Type IB	YP_170840 *Synechococcus elongatus* PCC_6301	E	T	N	K	K	G	D	F	K	D	E	H	R	H	K	S	G	G	G
Type II	P50922 *Rhodobacter capsulatus* ATCC11166	E	T	N	K	K	G	D	F	K	D	E	H	R	H	K	S	G	G	G
Type II/III	YP_566926 *Methanococcoides burtonii* DSM_6242	E	T	N	K	K	G	D	F	K	D	E	H	R	H	K	S	G	G	S
Type III	AAB99239 *Methanocaldococcus jannaschii* DSM_2661	E	T	N	K	K	G	D	L	K	D	E	H	R	H	K	S	G	G	G
	BAD86479 *Thermococcus kodakaraensis* KOD1	E	T	N	K	K	G	D	Y	K	D	E	H	R	H	K	S	G	G	G
	OLS23198.1 *Ca.* Heimdallarchaeota archaeon LC_3 (HeimC3_25390)	E	T	N	K	K	G	D	V	K	D	E	H	R	H	K	S	G	G	G
	KKK43062.1 *Ca.* Lokiarchaeum sp. GC14_75 (Lokiarch_30170)	E	T	N	K	K	G	D	L	K	D	E	H	R	H	K	S	G	G	G
	OLS27808.1 *Ca.* Heimdallarchaeota archaeon LC_2 (HeimC2_10010)	E	T	N	K	K	G	T	W	K	D	E	H	R	H	K	S	G	G	G
	OLS31478.1 *Ca.* Heimdallarchaeota archaeon AB125 (HeimAB125_16260)	E	T	N	K	K	G	D	F	K	D	E	H	R	H	K	S	G	G	G
	OLS14054.1 *Ca.* Lokiarchaeota archaeon CR_4 (RBG13Loki_2232)	E	T	N	K	K	G	D	V	K	D	E	H	R	H	K	S	G	G	G
	OLS18291.1 *Ca.* Odinarchaeota archaeon LCB_4 (OdinLCB4_15300)	E	T	N	K	K	G	T	S	K	D	E	H	R	H	K	S	G	G	G
	OLS14417.1 *Ca.* Lokiarchaeota archaeon CR_4 (RBG13Loki_1973)	E	T	N	K	K	G	D	I	K	D	E	H	T	L	K	S	G	G	G
	KKK44923.1 *Ca.* Lokiarchaeum sp. GC14_75 (Lokiarch_14140)	E	T	N	K	C	G	D	V	K	D	E	H	M	V	K	S	G	G	G
	KKK45122.1 *Ca.* Lokiarchaeum sp. GC14_75 (Lokiarch_12480)	E	T	N	K	C	G	D	V	K	D	E	H	M	V	K	S	G	G	G
Type IV	KXH74397.1 *Ca.* Thorarchaeota archaeon SMTZ1-45 (AM325_06140)	E	T	N	K	C	Y	D	I	K	D	E	H	M	V	K	S	G	G	A
	KXH71633.1 *Ca.* Thorarchaeota archaeon SMTZ1-83 (AM324_08310)	E	T	N	K	C	Y	D	I	K	D	E	H	M	V	K	S	G	G	A
	OLS27625.1 *Ca.* Thorarchaeota archaeon AB_25 (ThorAB25_20030)*	E	T	N	K	C	Y	D	I	-	-	-	-	-	-	-	-	-	-	-
	CAB13232 *Bacillus subtilis subsp subtilis* str. 168	G	S	K	K	V	G	D	L	K	D	E	H	P	L	S	S	A	G	G

*partial

Suppl. Figure 18: Maximum likelihood phylogenetic analysis of ribulose-1,5-bisphosphate carboxylase/oxygenase (RuBisCO) and analysis of essential sites. a, Phylogenetic tree was estimated using IQ-tree LG+C60+R+F and is based on a protein alignment of 359 aligned sites and includes 171 sequences. All support values (SH-like approximate likelihood ratio test and ultrafast bootstraps) below 90 as well as support values of closely related sequences were removed to increase readability and are represented by filled circles according to the color code in the figure legend. Scale bar indicates number of substitutions per site. b, Alignment positions of active site residues[69] present in Asgard homologues as compared to representative species for each known RuBisCO-type. Amino acids, which are given as single-letter IUPAC code, are numbered according to *Synechococcus elongatus* PCC 6301 reference sequence. Raw data files are available via figshare (see Data availability for more details).

Suppl. File 1: Phylogenetic analyses of universal marker proteins. Maximum-likelihood analysis based on a concatenated set of 56 universal protein markers for archaeal representatives of all major clades (144 taxa, 6453 sites) using IQ-TREE under the LG+C60+F+G+PMSF model. The tree is rooted on the DPANN. Numbers at branches indicate bootstrap statistical support (100 replicates). Raw data files are available via figshare (see Data availability for more details).

(Heimdallarchaeote_AB_125:0.5119457884,((((((((((Candidatus_Bathyarchaeota_archaeon_B25:0.4531130314,Candidatus_Bathyarchaeota_archaeon_B24:0.4731823306)72:0.0400240000,miscellaneous_Crenarchaeota_group_archaeon_SMTZ_80:0.6020819648)67:0.0237290000,((miscellaneous_Crenarchaeota_group_6_archaeon_AD8_1:0.4186633848,(Candidatus_Bathyarchaeota_archaeon_B26_2:0.2162053929,(Candidatus_Bathyarchaeota_archaeon_BA2:0.1488715737,Candidatus_Bathyarchaeota_archaeon_BA1:0.1587608596)100:0.1023070000)75:0.0474330000)100:0.1125940000,((miscellaneous_Crenarchaeota_group_15_archaeon_DG_45:0.2178359671,Thaumarchaeota_archaeon_SCGC_AB_539_E09:0.2870999698)100:0.1023590000,Candidatus_Bathyarchaeota_archaeon_B23:0.2427957722)100:0.3052240000)100:0.0651900000)98:0.0659720000,(((((Cenarchaeum_symbiosum:0.2528176005,Nitrosopumilus_maritimus:0.1505108344)100:0.0882820000,Candidatus_Nitrosotenuis_cloacae:0.1798435586)100:0.0812630000,Candidatus_Nitrosotalea_devanaterra:0.1815256419)100:0.2647440000,(Ca_Nitrososphaera:0.0788246241,Nitrososphaera_viennensis_EN76:0.1004829283)100:0.2441430000)100:0.5402010000,((Aigarchaeota_archaeon_JGI_0000106_J15:0.3605721576,((Aigarchaeota_archaeon_OS1:0.0367179819,Aigarchaeota_archaeon_SCGC_AAA471_B22:0.0617268900)100:0.2609830000,Aigarchaeota_archaeon_SCGC_AAA471_E14:0.3729145924)100:0.1671580000)90:0.0451010000,Candidatus_Caldiarchaeum_subterraneum:0.4441103811)100:0.3178320000)98:0.0696250000)100:0.0619260000,(((Geoarchaeon_NAG1:0.2720989573,Geo_AAA471:0.2534452452)100:0.5434200000,(((Sulfolobus_acidocalcarius:0.2319193431,Metallosphaera_cuprina:0.2972266276)100:0.3617150000,(((Pyrolobus_fumarii:0.2051900286,Aeropyrum_pernix:0.4018732523)84:0.0565330000,Ignicoccus_hospitalis:0.3559141863)98:0.0452870000,Desulfurococcus_kamchatkensis:0.3921172805)100:0.0606660000)100:0.1281290000,(((Pyrobaculum_aerophilum:0.1815051956,Thermoproteus_uzoni:0.1880619751)100:0.1580240000,(Caldivirga_maquilingensis:0.3822967131,Vulcanisaeta_distri:0.2599948501)100:0.0723910000)100:0.2475740000,Thermofilum_pendens:0.4584292309)100:0.1184660000)84:0.0511610000)94:0.0320470000,((Candidatus_Methanosuratus_petracarbonis_V5:0.0090453197,Candidatus_Methanosuratus_petracarbonis_V4:0.0000026919)100:0.1482610000,((Candidatus_Methanomethylicus_mesodigestum_V1:0.0046958387,Candidatus_Methanomethylicus_mesodigestum_V2:0.0005984168)100:0.0441760000,Candidatus_Methanomethylicus_oleusabulum_V3:0.0368734041)100:0.1757180000)100:0.5020500000)99:0.0618830000)68:0.0321740000,((Kor1:0.5365366568,(Kor4_v2.filtered:0.3036017157,(Kor2:0.2238184972,Ca_Korarchaeum:0.2962272840)100:0.0724230000)100:0.1627930000)100:0.0883790000,Kor3:0.5793397151)100:0.2823680000)91:0.0414900000,(((((((((archaeon_GW2011_AR11:0.4966087548,archaeon_GW2011_AR3:0.4550070139)84:0.0782380000,(archaeon_GW2011_AR4:0.5813326123,archaeon_GW2011_AR15:0.5035291483)62:0.0530790000)69:0.0369600000,archaeon_GW2011_AR9:0.7132641404)100:0.1073650000,((archaeon_GW2011_AR20:0.4855603253,Nanoarchaeota_archaeon_SCGC_AAA011_G17:0.4730819495)70:0.0793580000,(archaeon_GW2011_AR17:0.6073917730,archaeon_GW2011_AR18:0.6214375403)59:0.0442480000)100:0.0620860000)99:0.0789890000,(((archaeon_GW2011_AR13:0.3102680013,archaeon_GW2011_AR19:0.3025266702)42:0.0354230000,Nanoarchaeota_archaeon_SCGC_AAA011_D5:0.2702275719)100:0.5334460000,archaeon_GW2011_AR6:0.6534922299)100:0.3003840000)100:0.0955910000,(Nanoarchaeum_equitans_Kin4_M:0.5414425351,Candidatus_Nanopusillus_acidilobi:0.7000242570)100:0.3461100000)94:0.0483270000,Candidatus_Parvarchaeum_acidiphilum_ARMAN_4:1.4189863069)100:0.0545450000,(((((Nanohaloarchaea_archaeon_SG9:0.1948546983,(Nanohaloarchaea_archaeon_PL_Br10_U2g27:0.1570703854,(Nanohaloarchaea_archaeon_B1_Br10_U2g29:0.1299062234,Candidatus_Haloredivivus_sp_G17:0.1448038422)69:0.0368570000)100:0.1222030000)89:0.0362240000,Candidatus_Nanosalina_sp_J07AB43:0.2904755147)96:0.0364810000,(Nanohaloarchaea_archaeon_PL_Br10_U2g16:0.1879147201,Nanohaloarchaea_archaeon_B1_Br10_U2g1:0.1747657297)100:0.0640860000)96:0.0780700000,Candidatus_Nanosalinarum_sp_J07AB56:0.4245938503)100:0.8025340000,(archaeon_GW2011_AR5:0.7784679340,((Candidatus_Aenigmarchaeota_archaeon_JGI_0000106_F11:0.3480567321,Candidatus_Micrarchaeota_archaeon_RBG_16_49_10:0.4891597952)1

00:0.2345570000,(Candidatus_Aenigmarchaeum_subterraneum_SCGC_AAA011_O16:0.4175100808,Candidatus_Micrarchaeota_archaeon_RBG_16_36_9:0.3305634076)100:0.3070420000)87:0.0558810000)100:0.1104580000)100:0.0636050000)96:0.0381950000,(((((archaeon_GW2011_AR21:0.3689632658,Diapherotrites_archaeon_SCGC_AAA011_K09_6G:0.4743490602)73:0.0589080000,Diapherotrites_archaeon_SCGC_AAA011_N19_5G:0.5635857648)42:0.0606430000,archaeon_GW2011_AR10:0.4108879722)46:0.0932110000,Nano_AAA011:0.4849340888)100:0.4424210000,Candidatus_Micrarchaeum_acidiphilum_ARMAN_2:1.3613198185)97:0.0834780000)100:0.0494900000,(((Candidatus_Altiarchaeales_archaeon_IMC4:0.4270153522,Candidatus_Altiarchaeales_archaeon_WOR_SM1_SCG:0.3334887534)97:0.0733080000,Candidatus_Altiarchaeales_archaeon_WOR_SM1_86_2:0.3783174389)100:0.0978190000,(Candidatus_Altiarchaeum_sp_CG2_30_32_3053:0.1037902554,Altiarchaeum_SM1_MSI:0.1029317431)100:0.7956100000)100:0.2627390000)100:0.0383750000,(((((Hadesarchaea_archaeon_YNP_45:0.2456273360,Hadesarchaea_archaeon_DG_33:0.1787536205)99:0.0645250000,(Hadesarchaea_archaeon_DG_33_1:0.2448048479,Hadesarchaea_archaeon_YNP_N21:0.2000892364)70:0.0312690000)100:0.3482460000,(((Arc_I_group_archaeon_B15fssc0709_Meth_Bin003:0.0448513845,Arc_I_group_archaeon_U1lsi0528_Bin089:0.1083845831)100:0.4109600000,Thermoplasmatales_archaeon_DG_70:0.4393983001)100:0.1433250000,(Pyrococcus_furiosus:0.0807378113,Thermococcus_kodakarensis:0.0883115265)100:0.3189490000)99:0.0461040000)79:0.0271940000,((Methanococcus_maripaludis:0.3305886271,Methanocaldococcus_jannaschii:0.1743835270)100:0.2712160000,(((Methanosphaera_stadtmanae:0.2717423870,Methanobacterium_AL:0.1476723137)100:0.0955320000,Methanothermobacter_thermauto:0.1126648235)100:0.1433530000,Methanothermus_ferv:0.1821868526)100:0.2012670000)87:0.0430680000)94:0.0305370000,(((((Methanosaeta_thermophila:0.3907974225,(Methanosarcina_acetivorans:0.3460832542,Candidatus_Methanoperedens_nitroreducens:0.3492219008)100:0.0618860000)99:0.0514910000,(Methanocella_paludicola:0.4338084092,((Methanocorpusculum_labreanum:0.3378774428,(Methanoculleus_marisnigri:0.2102787828,Methanoplanus_petrolearius:0.2290565846)98:0.0573700000)100:0.2484840000,(Haloferax_volcanii:0.1741280583,Haloarcula_marismortui:0.1836330649)100:0.5455300000)86:0.0553610000)45:0.0320800000)63:0.0456490000,(uncultured_archaeon_ANME_1:0.4963718545,(Candidatus_Syntrophoarchaeum_caldarius:0.1397866544,Candidatus_Syntrophoarchaeum_butanivorans:0.0980292217)100:0.2650430000)100:0.0776360000)100:0.0971060000,(Ferroglobus_placidus:0.1241508911,Archaeoglobus_fulgidus:0.1685411238)100:0.3091740000)100:0.0799120000,(((Thermoplasma_acidoph:0.2832671403,Ferroplasma_acidarmanus:0.3767134251)100:0.4018670000,Aciduliprofundum_boonei:0.2991713160)100:0.1175000000,(Methanomassiliicoccus:0.4740189710,(Thermoplasmatales_archaeon_SM1_50:0.2641616620,Thermoplasmatales_archaeon_SG8_52_3:0.2039809914)100:0.2867050000)91:0.0846780000)100:0.1363960000)100:0.0738590000)96:0.0268940000)100:0.1050430000)78:0.0342760000,((((Thorarchaeote_AB_25:0.0529313888,(Thor45:0.0204144184,Candidatus_Thorarchaeota_archaeon_SMTZ_45:0.0327720733)100:0.0398360000)100:0.0750040000,Thor83:0.1320739741)100:0.5338300000,Odinarchaeote_LCB4:0.5164121338)94:0.0433970000,(Lokiarchaeum_GC14_75:0.6968888177,Lokiarchaeote_CR_4:0.5709798690)100:0.2487610000)100:0.0504240000)90:0.0310000000,(((((Plasmodium_falciparum:0.3641438771,Tetrahymena_thermophila:0.5012707949)82:0.0567880000,((((Chlamydomonas_reinhardtii:0.1853510417,Arabidopsis_tha:0.1649083532)100:0.0845610000,(Bigelowiella_natans:0.3482763535,Tpseudonana:0.3345170553)87:0.0440040000)76:0.0255950000,(Saccharomyces_cerev:0.3515848858,Homo_sapiens:0.1965011570)99:0.0527320000)51:0.0275410000,(Dictyostelium_dis:0.3371247249,Thecamonas_trahens:0.3295523016)55:0.0424430000)84:0.0365720000)66:0.0352300000,(Naegleria_gruberi:0.4297535442,Leishmania_infantum:0.5017477514)77:0.0569910000)68:0.0588530000,Entamoeba_histolytica:0.4846889392)100:0.1100600000,Trichomonas_vaginalis:0.6764020263)100:0.9057540000)100:0.0804370000,(Heimdallarchaeote_LC_3:0.6004704979,SChinaSea_Heimdall:0.4926646175)100:0.2158920000)100:0.1665880000,Heimdallarchaeote_LC_2:0.7012944200);

Suppl. File 2: Phylogenetic analyses of universal marker proteins after removal of fast evolving sites. Maximum-likelihood analysis is based on a concatenated set of 56 universal protein markers, after removal of the fastest-evolving sites (144 taxa, 5020 sites) using IQ-TREE under the LG+C60+F+G+PMSF model. Numbers at branches indicate bootstrap statistical support (100 replicates). Raw data files are available via figshare (see Data availability for more details).

(Heimdallarchaeote_AB_125:0.2928752461,(((((((Candidatus_Bathyarchaeota_archaeon_B25:0.2576332972,Candidatus_Bathyarchaeota_archaeon_B24:0.2526796273)96:0.019728,miscellaneous_Crenarchaeota_group_archaeon_SMTZ_80:0.3263807535)95:0.017056,(((miscellaneous_Crenarchaeota_group_6_archaeon_AD8_1:0.2367516196,(Candidatus_Bathyarchaeota_archaeon_BA2:0.0861171418,Candidatus_Bathyarchaeota_archaeon_BA1:0.0974642542)100:0.047737)87:0.023556,Candidatus_Bathyarchaeota_archaeon_B26_2:0.1161076513)100:0.071130,((miscellaneous_Crenarchaeota_group_15_archaeon_DG_45:0.1238104185,Thaumarchaeota_archaeon_SCGC_AB_539_E09:0.1504660449)100:0.064200,Candidatus_Bathyarchaeota_archaeon_B23:0.1406423645)100:0.168348)100:0.033258)96:0.032607,(((((Cenarchaeum_symbiosum:0.1423967759,Nitrosopumilus_maritimus:0.0880727544)100:0.052961,Candidatus_Nitrosotenuis_cloacae:0.1066986373)100:0.053142,Candidatus_Nitrosotalea_devanaterra:0.1108124325)100:0.154594,(Ca_Nitrososphaera:0.0414908913,Nitrososphaera_viennensis_EN76:0.0603424390)100:0.142028)100:0.298809,((Aigarchaeota_archaeon_JGI_0000106_J15:0.1885502863,((Aigarchaeota_archaeon_OS1:0.0262797011,Aigarchaeota_archaeon_SCGC_AAA471_B22:0.0432531308)100:0.143105,Aigarchaeota_archaeon_SCGC_AAA471_E14:0.2030318584)100:0.092678)97:0.025985,Candidatus_Caldiarchaeum_subterraneum:0.2432666605)100:0.195677)95:0.038464)100:0.038334,(((Kor1:0.2881651482,(Kor4_v2.filtered:0.1742037378,(Kor2:0.1284213180,Ca_Korarchaeum:0.1586226874)100:0.038116)100:0.101010)100:0.057113,Kor3:0.3103890041)100:0.167677,(((Geoarchaeon_NAG1:0.1550803276,Geo_AAA471:0.1430709836)100:0.300106,(((Sulfolobus_acidocalcarius:0.1334921306,Metallosphaera_cuprina:0.1644045996)100:0.204357,(((Pyrolobus_fumarii:0.1178680447,Aeropyrum_pernix:0.2278035065)97:0.030335,Ignicoccus_hospitalis:0.2079668745)100:0.024511,Desulfurococcus_kamchatkensis:0.2350887965)100:0.036425)100:0.080812,(((Pyrobaculum_aerophilum:0.1043569862,Thermoproteus_uzoni:0.1135277736)100:0.093661,(Caldivirga_maquilingensis:0.2147770111,Vulcanisaeta_distri:0.1517204874)100:0.039938)100:0.143774,Thermofilum_pendens:0.2432647327)100:0.067185)95:0.026303)99:0.015357,((Candidatus_Methanosuratus_petracarbonis_V5:0.0063215991,Candidatus_Methanosuratus_petracarbonis_V4:0.0000025546)100:0.076680,((Candidatus_Methanomethylicus_mesodigestum_V1:0.0028693107,Candidatus_Methanomethylicus_mesodigestum_V2:0.0001875353)100:0.027948,Candidatus_Methanomethylicus_oleusabulum_V3:0.0177341150)100:0.095345)100:0.270462)99:0.029900)83:0.019305)98:0.029100,(((((Thorarchaeote_AB_25:0.0297522209,(Thor45:0.0124677315,Candidatus_Thorarchaeota_archaeon_SMTZ_45:0.0197536180)100:0.022932)100:0.037425,Thor83:0.0795752878)100:0.288900,Odinarchaeote_LCB4:0.2786545193)88:0.018743,(Lokiarchaeum_GC14_75:0.4027761540,Lokiarchaeote_CR_4:0.3345673018)100:0.139449)100:0.025326,(((((Plasmodium_falciparum:0.2085223709,Tetrahymena_thermophila:0.3194920166)73:0.034773,(((Chlamydomonas_reinhardtii:0.1102354254,Arabidopsis_tha:0.0993637014)100:0.055215,(Bigelowiella_natans:0.2053383662,Tpseudonana:0.2066663550)99:0.028938)79:0.016541,((Saccharomyces_cerev:0.2156302829,Homo_sapiens:0.1224174531)94:0.027732,(Dictyostelium_dis:0.2083541297,Thecamonas_trahens:0.2008817613)62:0.024938)61:0.014422)96:0.024404)68:0.020668,(Naegleria_gruberi:0.2690815171,Leishmania_infantum:0.3024806769)78:0.030179)74:0.039396,Entamoeba_histolytica:0.2968605001)100:0.078008,Trichomonas_vaginalis:0.4194799783)100:0.524230)42:0.010032)67:0.016736,((((((((((archaeon_GW2011_AR11:0.2704708130,archaeon_GW2011_AR3:0.2570247121)96:0.040935,(archaeon_GW2011_AR4:0.3186664594,archaeon_GW2011_AR15:0.2948153160)92:0.029914)100:0.021840,archaeon_GW2011_AR9:0.4048077455)100:0.065613,((archaeon_GW2011_AR20:0.2871980917,Nanoarchaeota_archaeon_SCGC_AAA011_G17:0.2795197136)79:0.046001,(archaeon_GW2011_AR17:0.3455077894,archaeon_GW2011_AR18:0.3572807861)79:0.029573)100:0.029174)100:0.047009,((archaeon_GW2011_AR13:0.1784562909,(Nanoarchaeota_archaeon_SCGC_AAA011_D5:0.1652680619,archaeon_GW2011_AR19:0.1846220301)98:0.027684)100:0.316135,archaeon_GW2011_AR6:0.3757921568)100:0.178003)100:0.060528,(Nanoarchaeum_equitans_Kin4_M:0.3136124966,Candidatus_Nanopusillus_acidilobi:0.

4411257580)100:0.202730)100:0.029227,Candidatus_Parvarchaeum_acidiphilum_ARMAN_4:0.8461739376)100:0.034398,((((Nanohaloarchaea_archaeon_SG9:0.1132825771,(((Nanohaloarchaea_archaeon_PL_Br10_U2g27:0.0945141476,Nanohaloarchaea_archaeon_B1_Br10_U2g29:0.0838380440)99:0.026215,Candidatus_Haloredivivus_sp_G17:0.0857715585)100:0.076165,Candidatus_Nanosalina_sp_J07AB43:0.1706675622)100:0.023863)100:0.033432,(Nanohaloarchaea_archaeon_PL_Br10_U2g16:0.1121395047,Nanohaloarchaea_archaeon_B1_Br10_U2g1:0.1105100764)100:0.042800)100:0.045492,Candidatus_Nanosalinarum_sp_J07AB56:0.2737061602)100:0.451827,(archaeon_GW2011_AR5:0.4375157604,((Candidatus_Aenigmarchaeota_archaeon_JGI_0000106_F11:0.2039825969,Candidatus_Micrarchaeota_archaeon_RBG_16_49_10:0.2799267749)100:0.142718,(Candidatus_Aenigmarchaeum_subterraneum_SCGC_AAA011_O16:0.2597734948,Candidatus_Micrarchaeota_archaeon_RBG_16_36_9:0.2019659819)100:0.156027)99:0.035202)100:0.067332)100:0.042257)99:0.024786,((((archaeon_GW2011_AR21:0.2311695189,Diapherotrites_archaeon_SCGC_AAA011_K09_6G:0.2739890648)100:0.049886,(Diapherotrites_archaeon_SCGC_AAA011_N19_5G:0.3172921306,archaeon_GW2011_AR10:0.1888879368)85:0.037809)83:0.053895,Nano_AAA011:0.2673741530)100:0.263781,Candidatus_Micrarchaeum_acidiphilum_ARMAN_2:0.8154579369)100:0.053567)100:0.028880,(((Candidatus_Altiarchaeales_archaeon_IMC4:0.2342178374,Candidatus_Altiarchaeales_archaeon_WOR_SM1_SCG:0.1744397512)100:0.045033,Candidatus_Altiarchaeales_archaeon_WOR_SM1_86_2:0.2147362419)100:0.057120,(Candidatus_Altiarchaeum_sp_CG2_30_32_3053:0.0737814278,Altiarchaeum_SM1_MSI:0.0662605690)100:0.460538)100:0.150970)100:0.024629,(((((Hadesarchaea_archaeon_YNP_45:0.1432494873,Hadesarchaea_archaeon_DG_33:0.1088459762)95:0.036844,(Hadesarchaea_archaeon_DG_33_1:0.1417478473,Hadesarchaea_archaeon_YNP_N21:0.1134198622)93:0.017617)100:0.191723,(((Arc_I_group_archaeon_B15fssc0709_Meth_Bin003:0.0258586073,Arc_I_group_archaeon_U1lsi0528_Bin089:0.0781824935)100:0.213623,Thermoplasmatales_archaeon_DG_70:0.2300603898)100:0.082953,(Pyrococcus_furiosus:0.0457492873,Thermococcus_kodakarensis:0.0513814250)100:0.172184)100:0.028674)91:0.015003,((Methanococcus_maripaludis:0.1861893675,Methanocaldococcus_jannaschii:0.0968532236)100:0.147919,(((Methanosphaera_stadtmanae:0.1416960487,Methanobacterium_AL:0.0750576720)100:0.049283,Methanothermobacter_thermauto:0.0649599757)100:0.084065,Methanothermus_ferv:0.0986154825)100:0.110005)100:0.026342)100:0.014888,(((((Methanosaeta_thermophila:0.2028158404,(Methanosarcina_acetivorans:0.1957996843,Candidatus_Methanoperedens_nitroreducens:0.1845454941)100:0.030342)100:0.023981,(Methanocella_paludicola:0.2316270532,((Methanocorpusculum_labreanum:0.1799391639,(Methanoculleus_marisnigri:0.1103367772,Methanoplanus_petrolearius:0.1249728363)100:0.035637)100:0.133049,(Haloferax_volcanii:0.0986221119,Haloarcula_marismortui:0.1061408156)100:0.297410)100:0.030385)94:0.018797)93:0.024075,(uncultured_archaeon_ANME_1:0.2729942273,(Candidatus_Syntrophoarchaeum_caldarius:0.0710397049,Candidatus_Syntrophoarchaeum_butanivorans:0.0516405097)100:0.145365)100:0.033684)100:0.052239,(Ferroglobus_placidus:0.0706377564,Archaeoglobus_fulgidus:0.0940691233)100:0.166343)100:0.046167,(((Thermoplasma_acidoph:0.1594383260,Ferroplasma_acidarmanus:0.2068978205)100:0.220409,Aciduliprofundum_boonei:0.1534174837)100:0.062302,(Methanomassiliicoccus:0.2404226722,(Thermoplasmatales_archaeon_SM1_50:0.1508279051,Thermoplasmatales_archaeon_SG8_52_3:0.1149976575)100:0.159494)88:0.040828)100:0.071061)100:0.043855)99:0.018153)100:0.059263)100:0.063213,(Heimdallarchaeote_LC_3:0.3338784722,SChinaSea_Heimdall:0.2708131853)100:0.122024)100:0.093803,Heimdallarchaeote_LC_2:0.3898869217);

Suppl. File 3: Phylogenetic analyses of universal marker proteins after removal of DPANN archaea and fast evolving sites. Maximum-likelihood analysis was based on a concatenated set of 56 universal protein markers, after removal of the fastest-evolving sites, and excluding DPANN representatives (104 taxa, 5008 sites) using IQ-TREE under the LG+C60+F+G+PMSF model. Numbers at branches indicate bootstrap statistical support (100 replicates). Raw data files are available via figshare (see Data availability for more details).

(Heimdallarchaeote_AB_125:0.2753135815,(((((((((Candidatus_Bathyarchaeota_archaeon_B25:0.2336842229,Candidatus_Bathyarchaeota_archaeon_B24:0.2293072611)67:0.0160270000,miscellaneous_Crenarchaeota_group_archaeon_SMTZ_80:0.2994076157)74:0.0127260000,(((miscellaneous_Crenarchaeota_group_6_archaeon_AD8_1:0.2128375546,(Candidatus_Bathyarchaeota_archaeon_BA2:0.0791803903,Candidatus_Bathyarchaeota_archaeon_BA1:0.0856296015)100:0.0381420000)73:0.0221990000,Candidatus_Bathyarchaeota_archaeon_B26_2:0.1032920367)100:0.0643980000,((miscellaneous_Crenarchaeota_group_15_archaeon_DG_45:0.1119863372,Thaumarchaeota_archaeon_SCGC_AB_539_E09:0.1421864268)100:0.0560090000,Candidatus_Bathyarchaeota_archaeon_B23:0.1302738407)100:0.1560470000)100:0.0275500000)89:0.0293320000,(((((Cenarchaeum_symbiosum:0.1256062741,Nitrosopumilus_maritimus:0.0818520869)100:0.0505150000,Candidatus_Nitrosotenuis_cloacae:0.0941423095)100:0.0464360000,Candidatus_Nitrosotalea_devanaterra:0.1025858591)100:0.1463980000,(Ca_Nitrososphaera:0.0380180376,Nitrososphaera_viennensis_EN76:0.0535685788)100:0.1298000000)100:0.2821570000,((Aigarchaeota_archaeon_JGI_0000106_J15:0.1742193317,((Aigarchaeota_archaeon_OS1:0.0239533738,Aigarchaeota_archaeon_SCGC_AAA471_B22:0.0405684018)100:0.1294120000,Aigarchaeota_archaeon_SCGC_AAA471_E14:0.1869180340)100:0.0825500000)77:0.0228150000,Candidatus_Caldiarchaeum_subterraneum:0.2206140559)100:0.1817890000)89:0.0414090000)100:0.0343000000,(((Kor1:0.2651649861,(Kor4_v2.filtered:0.1575735627,(Kor2:0.1131258394,Ca_Korarchaeum:0.1404138858)100:0.0341560000)100:0.0928520000)100:0.0533280000,Kor3:0.2874064018)100:0.1528820000,(((Geoarchaeon_NAG1:0.1461450081,Geo_AAA471:0.1233876504)100:0.2902970000,(((Sulfolobus_acidocalcarius:0.1193094710,Metallosphaera_cuprina:0.1480239482)100:0.1867750000,(((Pyrolobus_fumarii:0.1042088633,Aeropyrum_pernix:0.2039007103)55:0.0248560000,Ignicoccus_hospitalis:0.1875035844)97:0.0215690000,Desulfurococcus_kamchatkensis:0.2113263888)99:0.0298950000)100:0.0732740000,(((Pyrobaculum_aerophilum:0.0949735492,Thermoproteus_uzoni:0.0994199202)100:0.0872270000,(Caldivirga_maquilingensis:0.1901766946,Vulcanisaeta_distri:0.1405652332)97:0.0358030000)100:0.1291230000,Thermofilum_pendens:0.2183540751)100:0.0622840000)58:0.0222840000)99:0.0148690000,((Candidatus_Methanosuratus_petracarbonis_V5:0.0054809690,Candidatus_Methanosuratus_petracarbonis_V4:0.0000025071)100:0.0713590000,((Candidatus_Methanomethylicus_mesodigestum_V1:0.0030118134,Candidatus_Methanomethylicus_mesodigestum_V2:0.0001516040)100:0.0244820000,Candidatus_Methanomethylicus_oleusabulum_V3:0.0163362919)100:0.0853660000)100:0.2470540000)95:0.0255920000)91:0.0168890000)96:0.0286730000,((((((Hadesarchaea_archaeon_YNP_45:0.1329479445,Hadesarchaea_archaeon_DG_33:0.0944241647)95:0.0303230000,Hadesarchaea_archaeon_DG_33_1:0.1319438479)57:0.0181990000,Hadesarchaea_archaeon_YNP_N21:0.1006370334)100:0.1755270000,((Methanococcus_maripaludis:0.1688536747,Methanocaldococcus_jannaschii:0.0900005940)100:0.1317540000,(((Methanosphaera_stadtmanae:0.1280112983,Methanobacterium_AL:0.0668465289)100:0.0462100000,Methanothermobacter_thermauto:0.0557823216)100:0.0769810000,Methanothermus_ferv:0.0877605990)100:0.1014160000)97:0.0197300000)53:0.0071820000,(((Arc_I_group_archaeon_B15fssc0709_Meth_Bin003:0.0232475234,Arc_I_group_archaeon_U1lsi0528_Bin089:0.0716052256)100:0.2018200000,Thermoplasmatales_archaeon_DG_70:0.2031773496)100:0.0804710000,(Pyrococcus_furiosus:0.0417240096,Thermococcus_kodakarensis:0.0458043458)100:0.1542150000)100:0.0297100000)84:0.0130200000,(((((Methanosaeta_thermophila:0.1834352438,(Methanosarcina_acetivorans:0.1801134713,Candidatus_Methanoperedens_nitroreducens:0.1705921165)90:0.0237020000)99:0.0214860000,(Methanocella_paludicola:0.2120856965,((Methanocorpusculum_labreanum:0.1658945587,(Methanoculleus_marisnigri:0.0959918219,Methanoplanus_petrolearius:0.1132098362)97:0.0292970000)100:0.1210410000,(Haloferax_volcanii:0.0895252802,Haloarcula_marismortui:0.0983743921)100:0.2730120000)95:0.0282950000)92:0.0181260000)96:0.0223730000,(uncultured_archaeon_ANME_1:0.2502074410,(Candidatus_Syntrophoarchaeum_caldarius:0.0652268066,Candidatus_Syntrophoarchaeum_buta

nivorans:0.0457084893)100:0.1295230000)98:0.0294570000)100:0.0477320000,(Ferroglobus_placidus:0.0624801670,Archaeoglobus_fulgidus:0.0835863236)100:0.1508200000)100:0.0397200000,(((Thermoplasma_acidoph:0.1478047480,Ferroplasma_acidarmanus:0.1871859881)100:0.2056740000,Aciduliprofundum_boonei:0.1391464850)100:0.0582040000,(Methanomassiliicoccus:0.2232765614,(Thermoplasmatales_archaeon_SM1_50:0.1345921651,Thermoplasmatales_archaeon_SG8_52_3:0.1101539943)100:0.1414890000)88:0.0409040000)100:0.0701090000)100:0.0369440000)100:0.0719980000)59:0.0121050000,(((Thorarchaeote_AB_25:0.0234233586,(Thor45:0.0107773770,Candidatus_Thorarchaeota_archaeon_SMTZ_45:0.0188485947)97:0.0200180000)100:0.0343690000,Thor83:0.0709674518)100:0.2760890000,(Odinarchaeote_LCB4:0.2535515008,(Lokiarchaeum_GC14_75:0.3908516406,Lokiarchaeote_CR_4:0.3151145991)100:0.1123350000)63:0.0096020000)99:0.0238650000)82:0.0165220000,((((Plasmodium_falciparum:0.1909199990,Tetrahymena_thermophila:0.2960092071)67:0.0273520000,((((Chlamydomonas_reinhardtii:0.1015493084,Arabidopsis_tha:0.0856689814)100:0.0444510000,(Bigelowiella_natans:0.1836013735,Tpseudonana:0.1914315382)88:0.0253360000)71:0.0161450000,((Saccharomyces_cerev:0.1956095640,Homo_sapiens:0.1085922128)83:0.0228620000,(Dictyostelium_dis:0.1917619524,Thecamonas_trahens:0.1844618962)48:0.0192750000)41:0.0124220000)61:0.0187360000,(Entamoeba_histolytica:0.2783573085,Leishmania_infantum:0.2891016899)65:0.0345450000)42:0.0132550000)52:0.0226570000,Naegleria_gruberi:0.2508036160)100:0.0697630000,Trichomonas_vaginalis:0.4057911732)100:0.5014970000)100:0.0401890000,(Heimdallarchaeote_LC_3:0.3151418784,SChinaSea_Heimdall:0.2473933463)100:0.1156070000)100:0.0862280000,Heimdallarchaeote_LC_2:0.3630172997);